# We are IntechOpen,
# the world's leading publisher of
# Open Access books
# Built by scientists, for scientists

## 6,900
Open access books available

## 185,000
International authors and editors

## 200M
Downloads

## 154
Countries delivered to

Our authors are among the

## TOP 1%
most cited scientists

## 12.2%
Contributors from top 500 universities

CLARIVATE ANALYTICS
**BOOK CITATION INDEX**
INDEXED

**WEB OF SCIENCE**™

Selection of our books indexed in the Book Citation Index
in Web of Science™ Core Collection (BKCI)

# Interested in publishing with us?
# Contact book.department@intechopen.com

# TEMPO-Mediated Oxidation of Lignocellulosic Fibers from Date Palm Leaves: Effect of the Oxidation on the Processing by RTM Process and Properties of Epoxy Based Composites

Adil Sbiai, Abderrahim Maazouz, Etienne Fleury,
Henry Sautereau and Hamid Kaddami

Additional information is available at the end of the chapter

http://dx.doi.org/10.5772/47763

## 1. Introduction

Lignocellulosic fibers display many well-known advantages as compared to their synthetic counterparts, including their being ecologically and toxicologically harmless, biologically degradable, and carbon dioxide ($CO_2$) neutral. Furthermore, natural fibers are characterized by a huge degree of variability and diversity in their properties. As they could be extracted from wood and annual plants, they are available in various forms, give a feeling of warmth to the touch, and have a pleasant appearance. None of these properties are offered by other non-wood engineering fibers.

Over the last two decades, a great deal of work has been dedicated to composites reinforced with natural fibers. Indeed the use of such natural product for the reinforcement of thermoplastic or thermosetting resins, leads to composites with lower density, higher specific stiffness and strength, together with a better biodegradability (Bledzki et al., 1999; Mishra et al., 2004; Zimmermann et al., 2004; Gandini, 2008). However, only few studies have dealt with polymers reinforced with lignocellulosic fibers obtained from palm trees (Abu-Sharkh and Hamid 2004; Wan Rosli et al. 2004; Kaddami et al. 2006; Bendahou et al. 2008 ; Sbiai et al. 2008; Bendahou et al. 2009). In the previous investigations (Kaddami et al. 2006; Bendahou et al. 2008; Sbiai et al. 2008), the reinforcing capability of palm tree fibers in thermoset or thermoplastic polymer matrices was demonstrated. In the case of epoxy-based composites, expected and strong interactions gave rise to enhanced mechanical and thermal characteristics. An increase in the glass transition temperature and an improvement of the thermo-mechanical properties, bending moduli, stress at break values, and maximum absorbed energies were

reported for composites based on fibers modified with acetic anhydride (Kaddami et al. 2006). The size of the fibers was also found to have an effect on the properties (Sbiai et al. 2008).

Reinforcement is the physical expression of the microscopic balance at the matrix/filler interface which makes up a filler network. Thus, the adhesion filler/matrix is the most important parameter governing reinforcement. It is required to render possible the transfer of mechanical constraints to the fiber when a load is applied to the composite. This adhesion can be enhanced through chemical or physical modification of the polymer and/or the filler. Such modifications depend on the physico-chemical nature of the matrix.

In most cases, the hydrophilic nature of the lignocellulosic fibers is detrimental for their interface interactions with common resins, which are mostly hydrophobic. Thus, chemical treatments have to be applied to overcome this issue (Reich et al., 2008). For this purpose, various surface modifications have been devised to selectively replace hydroxyl functions with hydrophobic groups (Duanmu et al., 2007; Biagiotti et al., 2004; Goussé et al., 2004; Gandini, 2008). Coupling agents giving rise to covalent junctions between the fibers and the matrix have also been described (Abdelmouleh et al., 2002; Paunikallio et al., 2006; Gonzalez-Sanchez et al., 2008; Bendahou et al., 2008).

Among modifications used to improve interfacial adhesion in natural fiber/polymer composites, oxidative treatments have received much attention during the seventies and eighties. Corona and plasma treatments were found to effectively enhance the interface in epoxy-based composites (Sakata et al 1993a,b), and chemical oxidative treatments have been widely reported in several studies for numerous composites of natural fiber and polymers. Many types of oxidants have been employed, e.g. dichromate/oxalic acid, ozone, potassium ferricyanide, ferric chloride, nitric acid, hydrogen peroxide, dicumyle peroxide, etc. (Sapieha et al 1989; Felix et al 1994; Cousin et al 1989; Kaliński et al. 1981; Raj et al. 1990; Felix and Gatenholm 1991; Flink et al. 1988; Young 1978; Moharana et al. 1990; Gardinera and Cabasso 1987; Zang and Sapieha 1991; Iwakura et al. 1965; Jutier et al. 1988; Michell et al. 1978; Coutts and Campbell 1979; Tzoganakis et al. 1988; Sung et al. 1982; Philippou et al. 1982; Manrich et al. 1989; Sapieha et al. 1991).

More recently, 2,2,6,6-tetramethylpiperidine-1-oxyl radical (TEMPO)-mediated oxidation of polysaccharides bearing primary alcohols has been intensively studied. This type of oxidation makes it possible to selectively oxidize, in aqueous medium, primary alcohol groups into carboxyl groups in natural polysaccharides (Isogai, and Kato 1998; Isogai and Saito 2005; Isogai et al. 2005; Davis and Flitsch 1993; De Nooy et al. 1995 Fukuzumi et al. 2009; Chang and Robyt 1996; Tahiri and Vignon 2000; Habibi et al. 2006).

Among composite processing techniques, resin transfer molding technique (RTM) has been widely used. This technique was used for high-performance air craft and automotive structures. This process can be divided into four stages: performing, mould filling, curing, and demoulding. First, the dry fiber preform is made and placed in the mould. The mould is filled with liquid resin which is then solidified in the curing stage. Note that the curing stage actually begins as soon as the resin is mixed. However, usually the process is designed such that cure proceeds slowly until the mould has been filled. Once cured, the part is removed

from the mould. In some cases, the part is demoulded before complete cure and post-cured in an oven. The purpose of this process was to improve the quality (dry spots, voids) and processability and to minimize the material wastage. In conventional fibers as glass fibers and carbon fibers when these fibers are presented in the form of bundles, the flow of resin through the preform is governed by two mechanisms: bulk flow and fiber wetting. Bulk flow occurs in the space between the fiber tows, whereas fiber wetting occurs within the fiber tows (O'Flynnet al 2007, Octeau 2001, Chu 2003). The interaction between matrix and reinforced fiber was particularly important to the RTM process (Nguen-Thuc et al 2004).

Many studies have been done on the kinetics of the polymerization systems epoxy / amine (Eloundou et al. 1996a and 1996b, Halley et al. 1996, Pichaud 1996, Pascault et al 2002, Nguen-Thuc et al 2004). The chemical reaction between the epoxy prepolymer and diamine hardener can lead, depending on the stoichiometry to formation of a network. It can occur during growth of the macromolecular chains, two structural transformations: gelation and vitrification. At the beginning of the reaction, when the glass transition temperature Tg is less than the reaction temperature, the reaction is controlled by chemical kinetics. At the gel point, the formation of macromolecular chains leads to a gelling phenomenon that characterizes the transition from a liquid to a rubbery state while the vitrification phenomenon reflects a shift from the rubbery state to glassy state (Eloundou et al. 1996a, Halley et al. 1996, Pascault et al 2002). At our knowledge no studies had been dedicated to the effect of the lignocellulosic fibers on the polymerization kinetic.

## 2. Part 1: TEMPO-mediated oxidation

### 2.1. Experimental section

#### 2.1.1. Materials

Leaflets from palm leaves of *P. dactylifera* were cut into pieces with lengths of 3 to 5 cm. After 24 h soxhlet extraction with acetone/ ethanol (75/25 by vol), the resulting product was slightly discolored. It was then ground and sieved in order to eliminate the fine powder and to keep only the particles with length ranging from 2 to 10 mm and widths from 0.2 to 0.8 mm. this material is hereafter called lignocellulosic fibers from date palm leaflets or DPLF. For XRD analysis, the samples were ground again to obtain a fine powder.

Cellulose, lignin and hemicellulose were extracted from the DPLF according to a previously described procedure (Bendahou et al., 2007). Cellulose whiskers were prepared from the rachis of *P. dactylifera* leaves (Bendahou et al., 2009).

2,2,6,6-tetramethylpiperidine-1-oxyl radical (TEMPO), sodium bromide, and 10% sodium hypochlorite solution were purchased from Sigma-Aldrich and used as received.

#### 2.1.2. General procedure for oxidative treatment (Gomez-Bujedo et al., 2004)

2g of DPLF were stirred in 200 mL distilled water for 1 min. TEMPO (32 mg, 0.065 mmol) and NaBr (0.636 g, 1.9 mmol) were dissolved in the suspension maintained at 4 °C. TEMPO-

mediated oxidation was initiated by adding dropwise the sodium hypochlorite solution (10 %, 32 ml, 43 mmol) and adjusting the pH at 10 by addition of a 0.1 M aqueous HCl. The suspension was then maintained at pH $10 \pm 0.5$ by continuous addition of 0.5 M NaOH and at 4 °C by means of a thermo-controlled bath. When the pH became stable, the reaction was quenched by adding methanol (5 mL). After neutralization of the reaction mixture to pH 7 by addition of 0.1M HCl, the suspension was filtrated and the solid particles were washed with distilled water and dried under vacuum at 30 °C for 18 hours. The soluble part was freeze-dried.

The same oxidation procedure was applied to the other samples, namely the cellulose, the hemicellulose and the lignin extracted from the DPLF, together with the cellulose whiskers extracted from the leave rachis.

### 2.1.3. Analysis techniques

The composition of the DPLF before and after oxidation *i.e.* the weight fraction of their cellulose, hemicellulose, and lignin contents was determined by selective extraction according to the NF T12-011 standard.

The carboxylate content of oxidized cellulose samples was determined by conductometric titrations (Saito & Isogai, 2004).

Infrared spectra were recorded on a FT-IR Perkin-Elmer 1720X spectrometer collecting 20 scans from 400 to 4000 cm$^{-1}$. Oxidized DPLF was converted to its acid form by ion exchange in order to displace the carboxyl absorption band toward higher wavelengths, thus eliminating any interference with the absorbed water band at 1640 cm$^{-1}$. Consequently the superposition of the sodium carboxylate peak with those of the hydrogen bonds could be avoided. The samples were dried with acetone and analyzed as KBr.

The XPS spectra were measured using an AXIS ULTRA DLD X-ray photoelectron spectrometer (KRATOS ANALYTICAL). Samples were dried at 50°C under vacuum during 24h, and set with conductive carbon adhesive tabs. The measurements were performed using a monochromatic Al K$\alpha$ X-ray with a pass energy of 160 eV and a coaxial charge neutralizer. The base pressure in the analysis chamber was smaller than 5×10-8 Pa. XPS spectra of O1s and C1s levels were measured at a normal angle with respect to the plane of the surface. High resolution spectra were corrected for charging effects by assigning a value of 284.6 eV to the C1s peak (adventitious carbon). Binding energies were determined with an accuracy of ±0.2 eV. The spectral decomposition of the C1s and O1s photoelectron peaks was carried out using a Shirley background at positions and FWHMs corresponding to known components, applying a 30% Lorentzian-to-Gaussian peak shape ratio.

The distribution of sodium and calcium ions present in a cross-section of the TEMPO-oxidized fibers was evaluated by the line analysis mode using an energy dispersive X-ray (EDX) device fitted into a scanning electron microscope (SEM) (Hitachi S3500 N). The X-ray detector was a Thermo Noran Superdry II having a resolution of 143eV. The analyses were performed without prior metallization of the samples.

A Philips X'Pert diffractometer equipped with a ceramic X-ray diffraction tube operated at 40 kV and 40 mA with CuKα radiation (wavelength 0.15418 nm) was used to determine the crystalline index of the specimens. The samples were compressed into disks using a cylindrical steel mould (Ø = 15 mm) with an applied pressure of 32 MPa. The diffracted intensity was recorded for 2θ angles in the range of 10 to 40°. Data were treated according to the empirical Segal method (Segal et al., 1959).

## 2.2. Results and discussion

### 2.2.1. TEMPO-mediated oxidation

DPLF samples were oxidized with TEMPO in aqueous medium. The experiments were performed (i) at low temperature (4 °C) to avoid the formation of side products and (ii) in the presence of a large quantity of sodium hypochlorite, i.e., 21 mmol per gram of the DPLF, in order to reach a high degree of oxidation (Montanari et al., 2005; Okita et al., 2009). The selective oxidation of a hydroxymethyl group to a carboxyl via an aldehyde requires two moles of NaOCl per mole of hydroxyl according to the known TEMPO mechanism (Figure 1) (De Nooy et al., 1995). The kinetic of the reaction was directly followed by addition of an aqueous NaOH solution which neutralizes the carboxylic acid functions resulting from the oxidation. Figure 2 clearly illustrates the efficiency of the reaction with a continuous increase in NaOH consumption over a period of 720 minutes. According to FTIR analysis on the water insoluble fraction (Figure 3), a stretching vibration C=O from the free COOH band near 1737 cm$^{-1}$ was seen to have a higher intensity in the case of oxidized fibers as opposed to their non-oxidized counterparts, thus providing evidence of the oxidation. Finally, as expected, the degree of oxidation (Do) was found to be 0.71 ± 0.02 (Table 1).
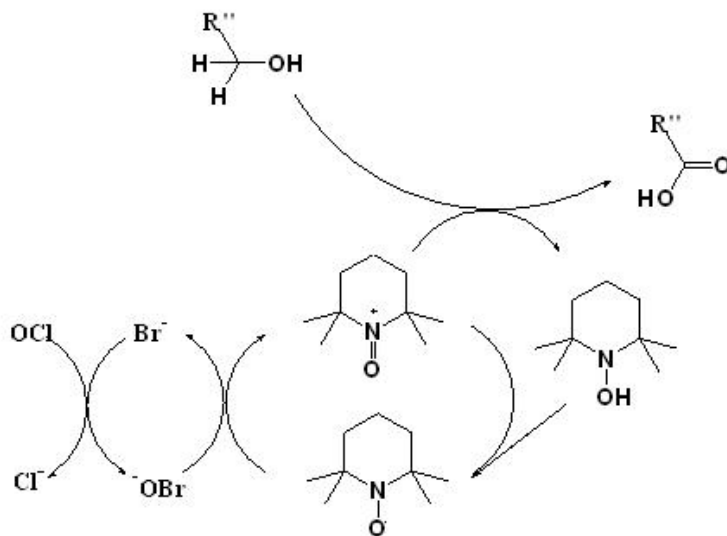


**Figure 1.** Scheme of the catalytic cycle for the oxidation of a primary hydroxyl.

The composition of DPLF was also investigated since a significant amount (30%) of the material became soluble in water during the oxidation. The results presented in Table 1 show that the proportions between components of DPLF have changed before and after the chemical

oxidative treatment. Thus cellulose content has increased from 35 to 46 %, whereas lignin and hemicelluloses contents have decreased. Nevertheless both lignin and hemicelluloses were still present in the oxidized DPLF at high concentration respectively 12 and 34 weight percent. Okita et al., have reported on a complete elimination of lignin and hemicelluloses in the case of TEMPO-mediated oxidation of thermomechanical softwood pulp under similar processing conditions (Okita et al., 2009). Pulp used by these authors contained similar percentage of lignin and hemicelluloses but was pried open by the mechanical refining process. One can thus deduce that thermomechanical pulps are much more reactive than lignocellulosic fibers having undergone no activation. On the other hand, a weak increase of the crystalline index is observed. This could be explained by the dissolution of the lignin after oxidation. Actually, this dissolution would induce a weak decrease of the intensity of the amorphous peak $I_{am}$ at $2\theta = 18°$ (Table 1 and supporting info S1).
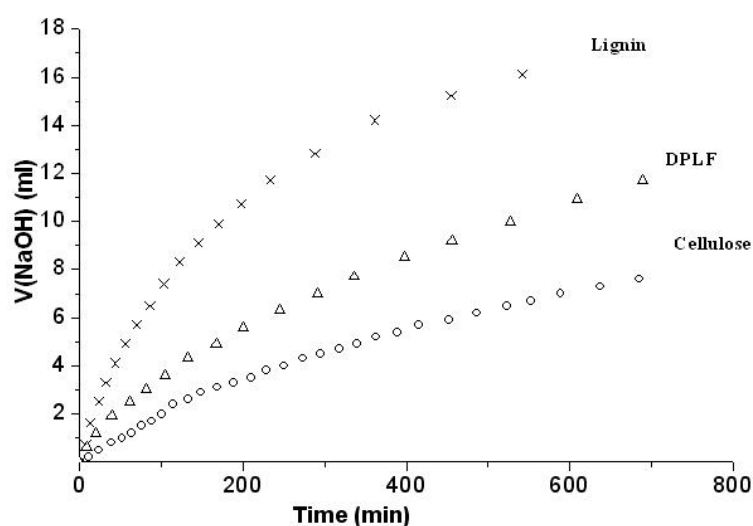


**Figure 2.** Kinetic TEMPO-mediated oxidation of DPLF, the extracted cellulose and lignin from DPLF: Consumption of the NaOH with the reaction time.

In order to compare the reactivity toward oxidation of each component of the DPLF, cellulose, hemicelluloses and lignin were extracted and subjected to the oxidation procedure. Kinetic data were recorded, except for hemicelluloses which presented very fast and uncontrollable kinetic. Data illustrated in Figure 2 clearly show that the extracted lignin reacted faster than the extracted cellulose, whereas the DPLF presented an intermediate rate. The structural characterization of the oxidized lignin and hemicellulose was not undertaken due to the complexity of possible structures. However, a previous study has shown that hemicelluloses extracted from the leaflets and rachis of the *P. dactylifera* palm consist of arabinoglucuronoxylans, which are either soluble or insoluble in hot water depending on the molar content of 4-O-methyl-glucuronic acid (Bendahou et al., 2007). One can thus deduce that the oxidative treatment under aqueous conditions allowed the conversion of the hydroxymethyl group of the arabinose moieties into carboxylic functions, which further facilitated the hemicellulose extraction in reaction medium maintained at 4°C. For lignin, the conversion of primary hydroxyl functions led to hydrosoluble products as already described (Okita et al., 2009).

| Samples | [COOH] mmol/g | Crystalline Index % | Composition Cellulose./ Hemicellulose./Lignin % | Water insoluble fraction % |
|---------|---------------|---------------------|-------------------------------------------------|----------------------------|
| Control DPLF | 0 | 49.5+/-0,5 | 35 / 28 / 27 | 100 |
| Oxidized DPLF | 0.71 | 52.5+/-0,5 | 46 / 34 / 12 | 70 |

**Table 1.** Chemical characterization of DPLF before and after TEMPO-mediated oxidation.

The reason for the moderate reactivity of the cellulose was already described. It originates from the crystalline nature of cellulose and from the difficulty to access to the hydroxyl groups at the surface of the cellulose crystals. In contrast, lignin and hemicelluloses, which are amorphous, react faster. The TEMPO-mediated oxidation of the cellulose sample was confirmed by the appearance of the characteristic carboxylic signal at 176 ppm in the ^{13}C CP-MAS NMR spectrum (Wikberg & Maunu, 2004; Martins et al., 2006) corresponding to a degree of oxidation (*Do*) equal to 0.07 (See supporting info S2 and S3).
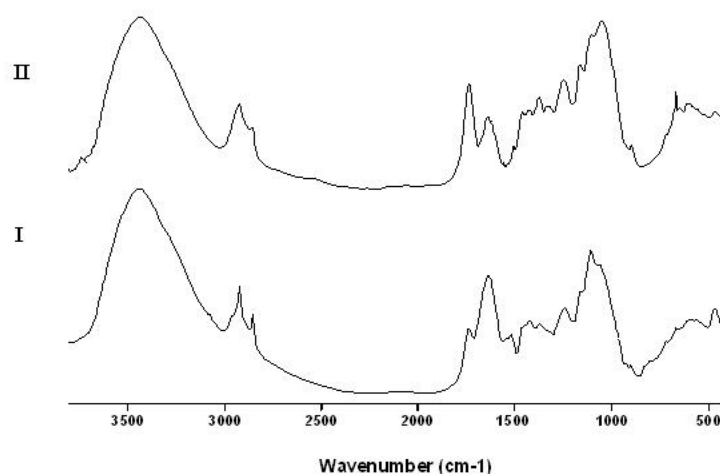


**Figure 3.** FT-IR spectra for DPLF before (I) and after TEMPO-mediated oxidation (II).

## 2.2.2. Heterogeneous kinetic modeling

Only few kinetic studies of TEMPO-mediated selective oxidation of cellulosic material have been reported in the literature (De Nooy et al., 1995; Sun et al., 2005; Mao et al., 2010). The authors have observed a first-order kinetic with respect to TEMPO and NaBr as well as a rate constant determined by their concentrations. It has also been claimed that the NaOCl concentration affects mainly the level of the conversion, leading to the possibility of reusing the reaction liquid by addition of more NaOCl. However, although TEMPO-mediated oxidation of cellulose corresponds to a reaction between a solid phase and a liquid phase, the heterogeneous aspect of the reaction was never envisaged.

In fact, cellulose fibers can be represented as accessible porous networks, where reagents can diffuse to the periphery of entities made up of bundles of cellulose microfibrils surrounded with lignin and/or hemicelluloses. This system can be described as a cylinder (Figure 4) with a diameter that becomes decreased when the Tempo-mediated oxidative process progresses.
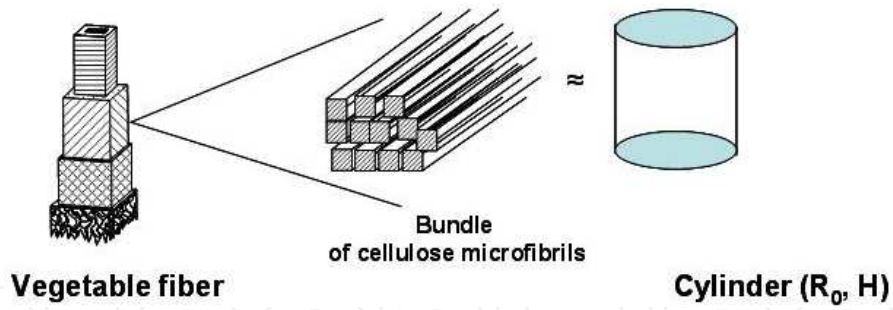
**Figure 4.** Schematization of the reactive substrate presented as a cylinder.

The interfacial specific rate $r_{is}$ of an heterogeneous reaction can be expressed by equation 1 where $R$ and $H$ are respectively the radius and the height of the cylinder and k the rate constant for a given temperature and concentration (Levenspiel, 1972).

$$r_{is} = 2\pi \, RH \, k \tag{1}$$

Considering $R_0$ as the initial radius, the conversion of the reaction at time $t$, is given by

$$X = \frac{R_0^2 - R^2}{R_0^2} \tag{2}$$

Since the initial molar concentration of the reactive function is $n_0$, its decrease with time can be described by equation 3:

$$dn = 2\pi \, R \, H \, r_{is} dt = n_0 dX = -\frac{2n_0}{R_0^2} R \, dR \tag{3}$$

Where:

$$dX = d(\frac{R_0^2 - R^2}{R_0^2})$$

Equation 3 can be simplified into:

$$dn = 2\pi H r_{is} dt = -\frac{2n_0}{R_0^2} dR$$

Which, after integration, gives the following relation:

$$R = R_0 - \frac{\pi \, H \, R_0^2 r_{is}}{n_0} t \tag{4}$$

By expressing the time required for a complete conversion to occurs as:

$$t_{Final} = \frac{n_0}{\pi \, H \, R_0 \, r_{is}}$$

and rearranging the relation, one obtains:

$$(1-X)^{1/2} = 1 - \frac{t}{t_{Final}} \qquad (5)$$

The conversion X was calculated from the evolution of the NaOH consumption given in Figure 2 and the evolution of $(1 - X)^{1/2}$ was plotted as a function of $t$. The results are presented in Figure 5, and as illustrated, the experimental values followed a linear equation as predicted by the model. The value of $t_{Final}$ calculated from the slope of the curves was $11 \times 10^3$ minutes.

Additional experiments were attempted, using cellulose whiskers extracted from the rachis of the from *P. dactylifera* palm. Here, the advantage was to have a pure cellulose substrate with a known length and a squarish cross-section. Consequently, the shape of the cellulose whiskers could be modeled as that of a cylinder (Elazzouzi-Hafraoui et al., 2008). The results presented in Figure 5 are also compatible with a heterogeneous model and clearly highlight that cellulose whiskers behave in a manner analogous to that of DPLF. However for the whiskers, the $t_{Final}$ was higher ($1.1 \times 10^4$ minutes) than for DPLF which caused the specific rate $r_{is}$ of the TEMPO-mediated oxidation to decrease. The difference can be ascribed to high reactivity of DPLF which contain lignin, hemicelluloses and amorphous cellulose being more reactive than cellulose whiskers.
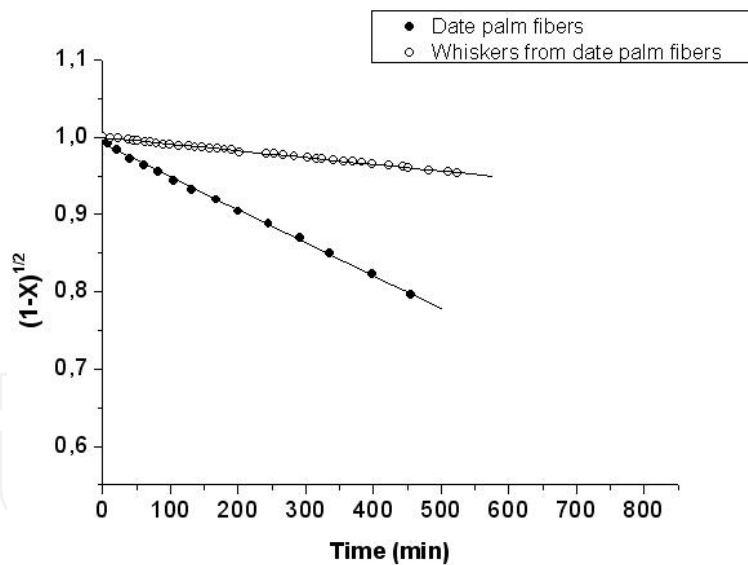


**Figure 5.** Modeling of the kinetics of TEMPO-mediated oxidation for (♦) DPLF: $(1-X)^{1/2} = 1 - 4,93 .10^{-4}t$ and (o) cellulose whiskers from data palm rachis: $(1-X)^{1/2} = 1 - 8,71 .10^{-5}t$.

### 2.2.3. Topological characterization

From the aforementioned model it can be inferred that the oxidation reaction occurs through a heterogeneous process. To characterize the topology of the chemical changes, X-rays photoelectron spectroscopy (XPS) and energy dispersive X-rays analysis were carried out on DPLF before and after oxidative treatment.

XPS revealed the modifications resulting from the oxidation (Figure 6). Indeed the C1s spectrum of the control product (spectrum a) consists of three major peaks at 284.6 (peak 1), 286.2 (peak 2) and 287.8 eV (peak 3), corresponding to C-C + C-H, C-O and O-C-O (and / or C=O) groups respectively. After oxidation (spectrum b), a new peak can be clearly distinguished at 288.8 eV and is attributed to the O=C-O function, typical of carboxylate group. This signal is overlapped with the one of the C=O group and is probably also present in the C1 spectrum of the control product but at lower level. In addition, a quantitative analysis indicates that the atomic concentration of non-oxidized carbon (peak 1) is of 71.2 % and 64.4 % before and after oxidation respectively. Assuming that XPS analysis only characterize a depth of 10 nm, these results clearly highlight that carboxylate functions are present at the top layers of DPLF.
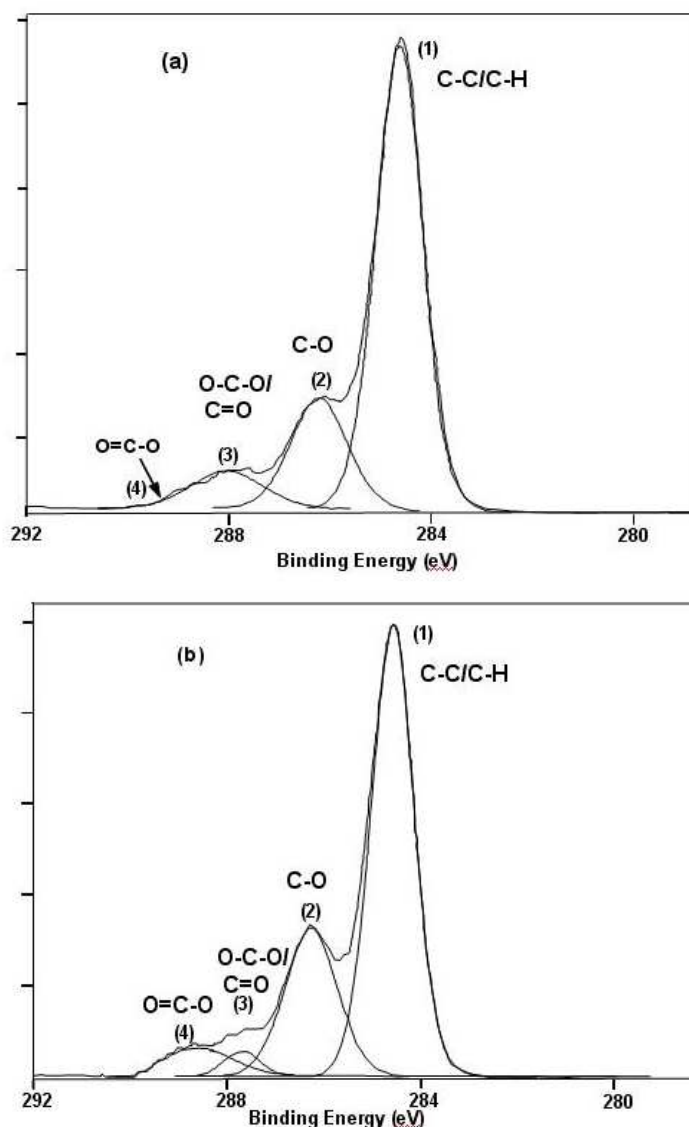


**Figure 6.** High resolution C1s spectra for DPLF (a) and after (b) TEMPO-mediated oxidation.

The location of carboxylate groups was clearly evidenced by the characterization with SEM/EDX analysis. In Figure 7 are represented typical cross-sections of DPLF showing also

the external wall of the fibers before oxidation (Figure 7a), after oxidation (Figure 7b) and after oxidation and calcium ions exchange (Figure 7c). Zones which are colored correspond to the location of the counter-ion of carboxylate functions. The more intense the coloration, the higher is the concentration of the counter-ion and therefore the carboxylate function.

Figure 7a shows the DPLF before oxidation and the coloration represents the mapping of sodium ions due to the presence of 4-O-methyl-glucuronic acid units within the raw fibers as mentioned above. The density of initial carboxylate is low in comparison to the one observed in the case of oxidized fibers (Figure 7b) indicating the success of the oxidation treatment. TEMPO-oxidized fibers treated within an aqueous calcium chloride solution led to fibers-COOCa$^+$ structures (Saito et al., 2005). As shown in Figure 7c, the density of calcium ion is high and comparable to that obtained with sodium.

It can also be noted that carboxylate groups are found to be slightly more dense at the surface of the fibers than inside, whereas the distribution at the surface is homogeneous and the one inside inhomogeneous. Such difference between the core and the surface which is confirmed with both mapping of calcium and sodium ions was never reported before.
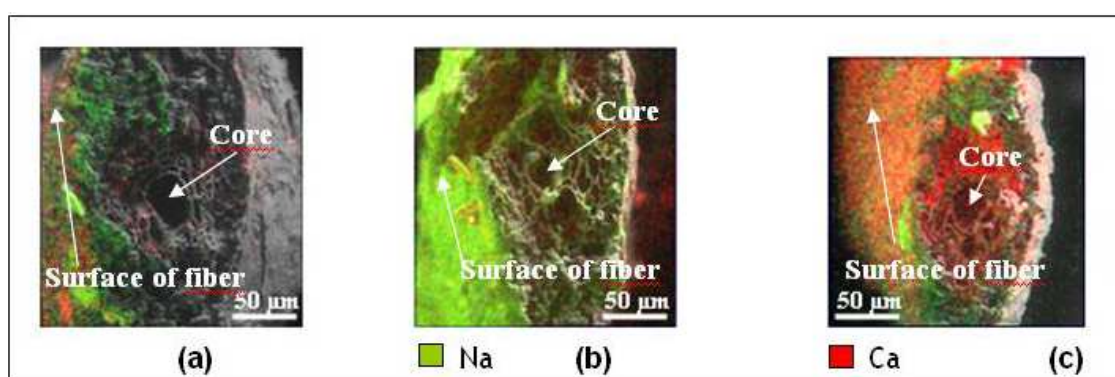


**Figure 7.** Energy dispersive X-ray analysis on fiber cross-section (a) before oxidation, (b) after oxidation, (c) after oxidation and ion-exchanged with CaCl$_2$. The colored parts correspond to the presence of the counter-ion of the carboxylate function: sodium in case of 7a and 7b and calcium in case of 7c.

This feature may be ascribed to the presence of hemicelluloses and lignin, which either limit the diffusion of the reagent within the fibers or –which is more probable - migrate to the surfaces after being oxidized. It is also important to underline that the morphology of the fibers remains identical after the TEMPO mediated-oxidation as shown in Figure 7.

## 3. Part 2: Effect of the oxidation on the processing by RTM process

### 3.1. Experimental section

#### 3.1.1. Materials

##### 3.1.1.1. Polymer matrix

The polyepoxy matrix was obtained through a polymerization reaction of an epoxy prepolymer with an amine curing agent. The selected epoxy resin was di-glycidyl ether of

bisphenol A (DGEBA) (Ref.: LY 556 ) supplied by Ciba-Geigy, and the curing agent was isophorone diamine (IPD) supplied by Fluka-Chemika. The characteristics of these components are presented in Table 2. The curing was carried out according to the following setup: 2 h at 80 °C, 2 h at 120 °C, and 2 h at 160 °C.
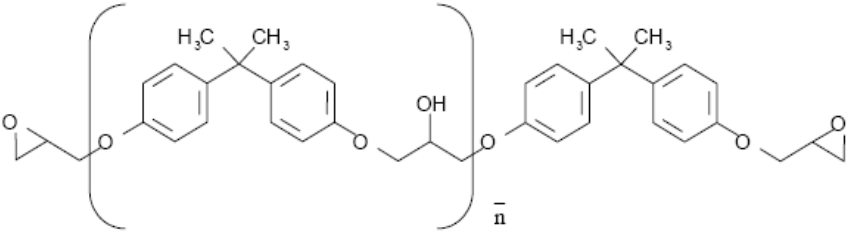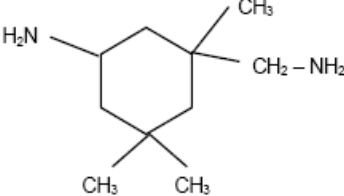
| Component | Chemical structure | Characteristics |
|---|---|---|
| Prepolymer DGEBA |  | Ciba Geigy LY 556 <br> n = 0.15 <br> M = 380 g/mol <br> d = 1.169 g/cm³ <br> f = 2 |
| isophorone diamine |  | Fluka–Chemika <br> M = 170 g/mol <br> d = 0.92 g/cm³ <br> g = 4 |

**Table 2.** Chemical characteristics

### 3.1.1.2. Reinforcement fiber preparation

The lignocellulosic fibers were obtained by cutting date palm tree leaves into small pieces of approximately 5 cm long and 10 mm wide. The fibers were then extracted for 24 h in a Soxhlet reflux of a solvent mixture composed of acetone/ethanol (75/25). Subsequently, the discolored fibers were dried at room temperature. The used fibers were denoted as unmodified. The length and width of these fibers ranged from 2 to 10 mm, and 0.2 to 0.8 mm, respectively. They were obtained by grinding and sieving the bleached fibers in a 0.1mm-hole sieve to eliminate particles designated as fines, after which they were further sieved through 0.8 mm holes to eliminate bigger fibers.

Fibers oxidation experiments were made under the following conditions. The following samples were oxidized separately. Samples (fiber, cellulose, lignin, and hemicellulose) (2 g, i.e., 12.35 mmol of anhydroglucose units) were dispersed in distilled water (200 ml) for 1 min with a mechanical agitator. TEMPO (32 mg, 0.065 mmol) and NaBr (0.636 g, 1.9 mmol) were added to the suspension, which was maintained at 4 °C. The sodium hypochlorite solution (10 %, 32.17 ml, 43.21 mmol) with pH adjusted to 10 by addition of a 0.1 M aqueous HCl was set at 4 °C by means a thermocontrolled bath. The mixture was then added to the suspension, which was stirred mechanically. The pH was maintained at 10 during the reaction by addition of a 0.5-M NaOH solution. The temperature of the suspension was maintained at 4 °C by means of a thermocontrolled bath during the oxidation reaction. When the reaction time exceeded 12 h, the kinetics became very slow and the solution turned a yellowish white. The reaction was stopped by adding 5 ml of methanol.

The reaction mixture was neutralized to pH 7 with 0.1 M HCl. The oxidized sample was washed with distilled water, after which it was filtered and dried at room temperature. The

fiber oxidation was characterized by various methods (IR, conductimetry, solid-state NMR, XPS, MEB, EDX, X-ray diffraction) (Sbiai and al 2010). In the following, the oxidized fibers are referred to as modified fibers.

### 3.1.1.3. Composite processing

Composites were processed using the resin transfer molding (RTM) method. This process can be divided into four stages: performing, mould filling, curing, and demoulding. The epoxy resin was stored in container A while container B contained the curing agent IPD. The resin mixtures were preheated at approximately 60 °C to reduce the viscosity. The resin was degassed for 20 min to prevent voids from forming during pumping. In container B, IPD was kept at room temperature under an argon atmosphere in order to avoid evaporation and carboxylation. A good circulation of the resin throughout the pump and pipes was necessary. A mold ($100 \times 60 \times 6$ mm$^3$) made of a composite material, was preheated at 80 °C for 2 h before injection. A continuous mat of date palm tree fibers (either unmodified or modified (oxidized)) used as reinforcement was placed in the mold cavity under isothermal conditions. To observe the flow of the resin during the injection process, a transparent mold made of glass was used under equivalent conditions. A camera was employed to observe the process, which was deemed to have come to an end when the resin was seen to exit from the vent at the other side of the mold. Upon completion of the cure cycle, the solid composite parts were ejected and post-cured under the same conditions as the pure matrices.

### 3.1.2. Analysis techniques

#### 3.1.2.1. Chemical composition of the fiber

The chemical compositions of the dried date palm tree fibers were determined according to French Standards (NFT12-011). It was thus possible to assess the weight fraction of cellulose, hemicelluloses, and lignin.

#### 3.1.2.2. Scanning Electron Microscopy (SEM)

SEM was used to investigate the morphology of the different types of materials, as well as the filler/matrix interface. The microscope was an ABT-55. The specimens were frozen in liquid nitrogen, fractured, mounted, coated with gold/palladium, and observed using an applied voltage of 10 kV.

#### 3.1.2.3. Differential Scanning Calorimetry (DSC)

A Mettler TA3000 calorimeter was used to measure the glass transition temperature, Tg, which was taken as the onset temperature of the specific heat increment. The heating rate was fixed at 10 °C min$^{-1}$, and scans were recorded under an argon atmosphere (flowrate10 mL min$^{-1}$) in a temperature range between -100 and +200 °C.

#### 3.1.2.4. Dynamic Mechanical Analysis (DMA)

DMA experiments were performed with a Rheometrics RDAII, equipped for rectangular samples and working in shear mode. Values of the shear storage, G′, and shear loss, G′′,

moduli as well as the tangent of the loss angle, $\tan\delta = G''/G'$, were determined. This apparatus was especially dedicated to the study of films and composite materials. The average typical dimensions of the composite samples were 20x4x1 mm³. The tests were performed under isochronal conditions at 1 Hz, and each sample was heated from -120 to +200 °C at a heating rate of 2K/min. The maximum shear strain was equal to 0.2%.

*3.1.2.5. Non-linear mechanical properties*

Three-point bending tests were performed according to the international ISO178 standard to determine the flexural strength (MPa), the flexural modulus (GPa), and the total absorbed energy (J) of the composites. The testing machine was a 2/M type supplied by MTS (load cell: 10kN). The samples were parallelepiped bars with dimensions close to 60x10x5 mm³ and the distance between the supports was fixed at 50 mm. Tests were carried out at room temperature, and the data collected on five samples was averaged.

## 3.2. Results and discussion

### 3.2.1. Chemical analysis of the fibers

Results of the chemical composition of the different fibers are presented in Table 3. It can be clearly seen that the chemical oxidation induced a significant decrease of the lignin content and an increase of that of the cellulose and hemicelluloses. This was explained by the oxidation followed by the dissolution of lignin during the TEMPO-mediated oxidation.

| Constituent | Raw dried palm tree fibers (wt %) | Oxidized fibers (wt %) |
|---|---|---|
| Cellulose | 35 % | 46 % |
| Hemicelluloses | 28 % | 34 % |
| Lignin | 27 % | 12 % |

**Table 3.** Chemical Composition of Date Palm Tree Fibers Before (raw dried palm tree fibers) and After (modified (oxidized) fibers) the Chemical Oxidative Treatment (Sbiai et al. 2010).

### 3.2.2. Observation of resin flow during composite preparation

With regard to the observation of front displacement in the mat during the RTM experiments, there was a large difference between the two kinds of fibers. In fact, in the case of unmodified fibers, the front displacement was slow and heterogeneous, whereas in the case of the oxidized fibers, it was faster and homogeneous. This difference is portrayed in Fig. 8, presenting the photos of the fronts taken after 15 seconds of resin injection. In fact, the distance covered by the resin front was higher in the case of the oxidized fibers. On the other hand, the mat of oxidized fibers was homogeneously traveled by the resin, as compared to the mat of unmodified fibers.

These differences could be explained by variations in compatibility between the resin and the filler in the two systems, giving rise to a difference of interaction at the resin/fiber interface. In fact, the carboxylic groups at the fiber surface, in addition to the low amount of lignin in the case of the modified fibers, helped increase the affinity of the epoxy resin with the oxidized

fibers. These observations were very important for the control of the process. On the other hand, one can predict some effects of the fiber oxidation on the morphologies and the properties.
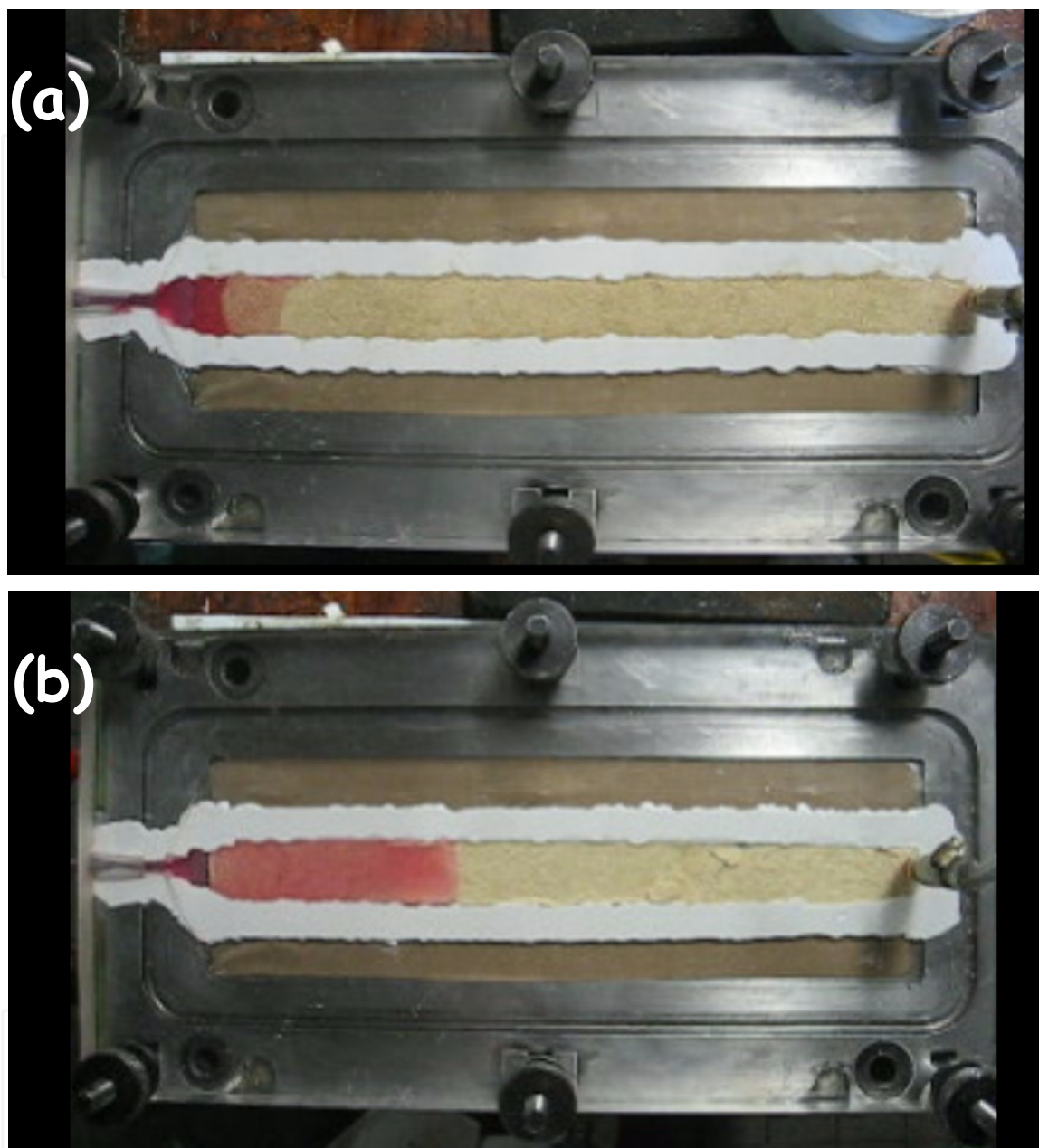


**Figure 8.** RTM experiment: the resin front after 15 second of injection (at T° = 25°C and P = 1.5 bar) on a mat of **(a)** unmodified and **(b)** TEMPO-mediated oxidized date palm tree fibers

### 3.2.3. Morphological investigation of the interfaces

Figures 9 and 10 show SEM micrographs of freshly fractured surfaces of composite materials based on the polyepoxy matrix filled with unmodified and modified fibers, respectively. Reinforced materials were investigated. For each composite material, at least tree magnifications were used to reveal the effect of the fiber treatment on the interfacial adhesion. For the unfilled material, i.e. the thermoset matrix (Fig 9-a), the fracture surface
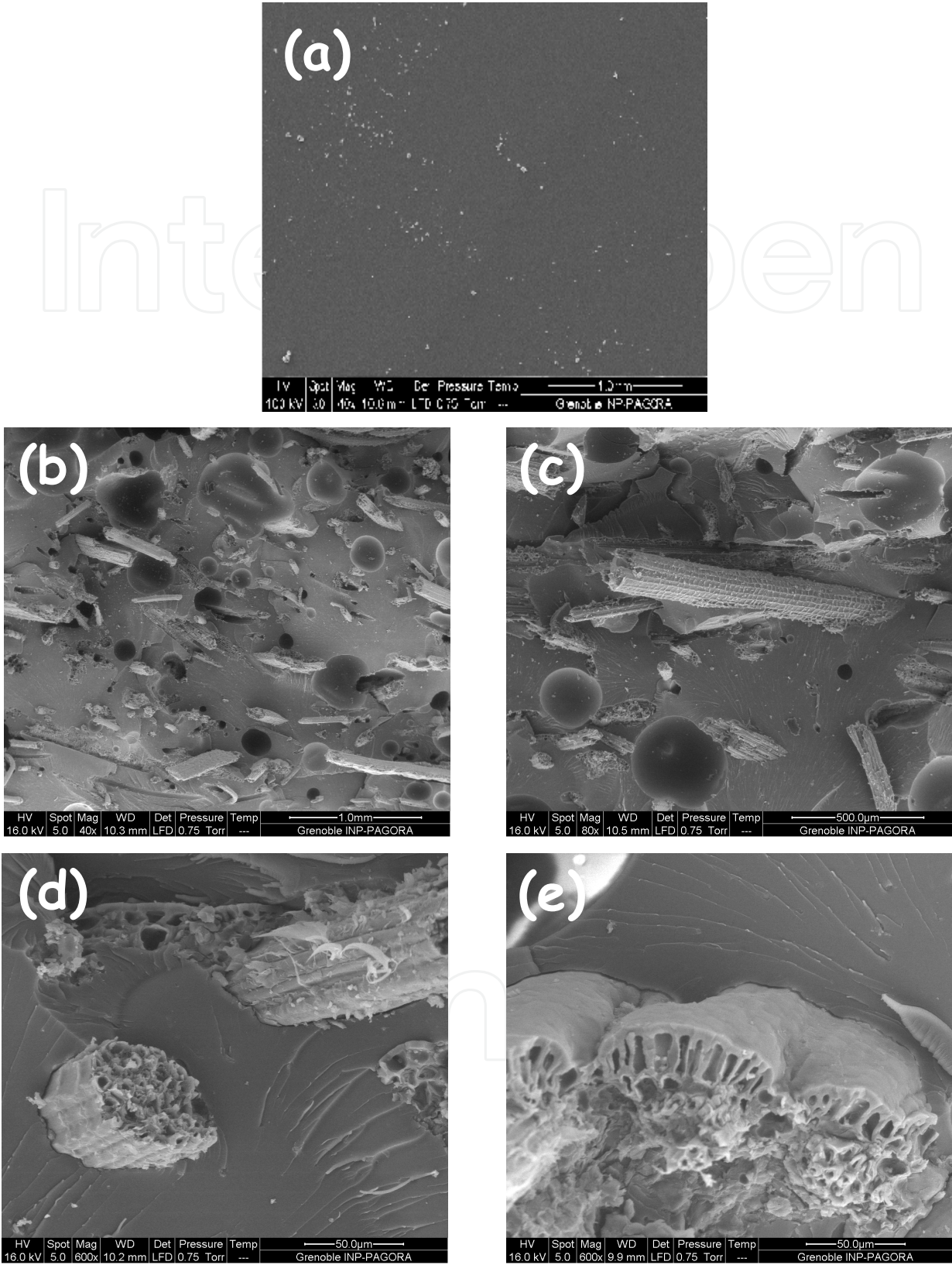
**Figure 9.** Scanning electron micrographs of freshly fractured surfaces of polyepoxy /unmodified fiber composites with (a) 0 wt%, and (b, c, d, e) 10 wt % of unmodified date palm tree fibers at various magnifications

was rather smooth, as could be expected for brittle polymers. By comparing these micrographs with those of the composite materials (Fig 9 b, c, d and e), the fibers could be clearly identified. The SEM micrographs in Fig. 9 indicated that the interfacial adhesion between the filler and the matrix was not very strong in the case of composites based on unmodified fibers. In fact, the fibers were pulled out from the matrix and their surface remained practically clean (see Figs 9-b and 9-c). On the other hand, fracturing the samples did not lead to the palm tree fibers breakage (Figs 9-d and 9-e). However, it is worth noting that the interaction between the unmodified fibers and the matrix was superior to that of the composite constituted of a hydrophobic matrix filled with unmodified fibers, such as unsaturated polyesters, polypropylenes or polyethylenes.

In contrast, for the composites containing modified fibers, the micrographs in Fig. 10 are evidence of a better adhesion between the matrix and the filler. One can observe the absence of holes around the fillers on the fractured surface, i.e. no debonding occurred. Nor was there any breakage of fibers during fracture (See Fig. 10-c and 10-d). On the other hand, the area surrounding the cellulosic filler seemed to be continuous with the matrix phase, and the epoxy resin appeared to be polymerized within the fiber lumens (see Figs. 10c and 10-d). This variation in interfacial adhesion between the composites based on unmodified and modified fibers is attributed to difference in the nature of physico-chemical interactions that can be created at the interface. This difference can be explained from the stronger interaction developed by the carboxylic groups created on the modified fibers. On the other hand, the dissolution of lignin after fiber oxidation gave rise to an increase of the hydrophilic character of the fibers. As a consequence, the wettability of the fiber surface with regard to the epoxy resin - a necessary condition for good interfacial adhesion - was superior in the case of the modified fibers. The introduction of the epoxy resin within the lumen was evidence of this higher thermodynamic affinity between the fibers and the polyepoxy matrix.

### 3.2.4. Thermal behavior of palm tree fiber-based composite materials

As mentioned above Section 2, the thermal behavior of date palm tree fiber-based composites was investigated by DSC. The glass transition temperatures, Tg's, of these materials are listed in Table 4. The Tg of the unfilled epoxy matrix was around 155°C. Table 3 clearly shows that the introduction of the lignocellulosic fibers led to a decrease in Tg. This decrease was more pronounced in the case of composites based on unmodified fibers.

The decrease in Tg could be explained by an unbalance of the stoichiometric ratio in the matrix as well as in the vicinity of the fibers after mixing with fibers. The fibers could have more affinity with one component as opposed to with another. This resulted in a hindering of the cross-linking process of the polyepoxy resin.

These results were completely opposite to those obtained in the case of composites based on an industrial epoxy matrix (DGEAB (AW106)/Jeffamin (HV953U)) supplied by CIBA – GEIGY. For the latter composites, an increase in Tg was observed after the introduction of the lignocellulosic filler (Kaddami et al 2006; Sbiai et al 2008). This difference could be attributed to the difference of resin and polymerization kinetics.
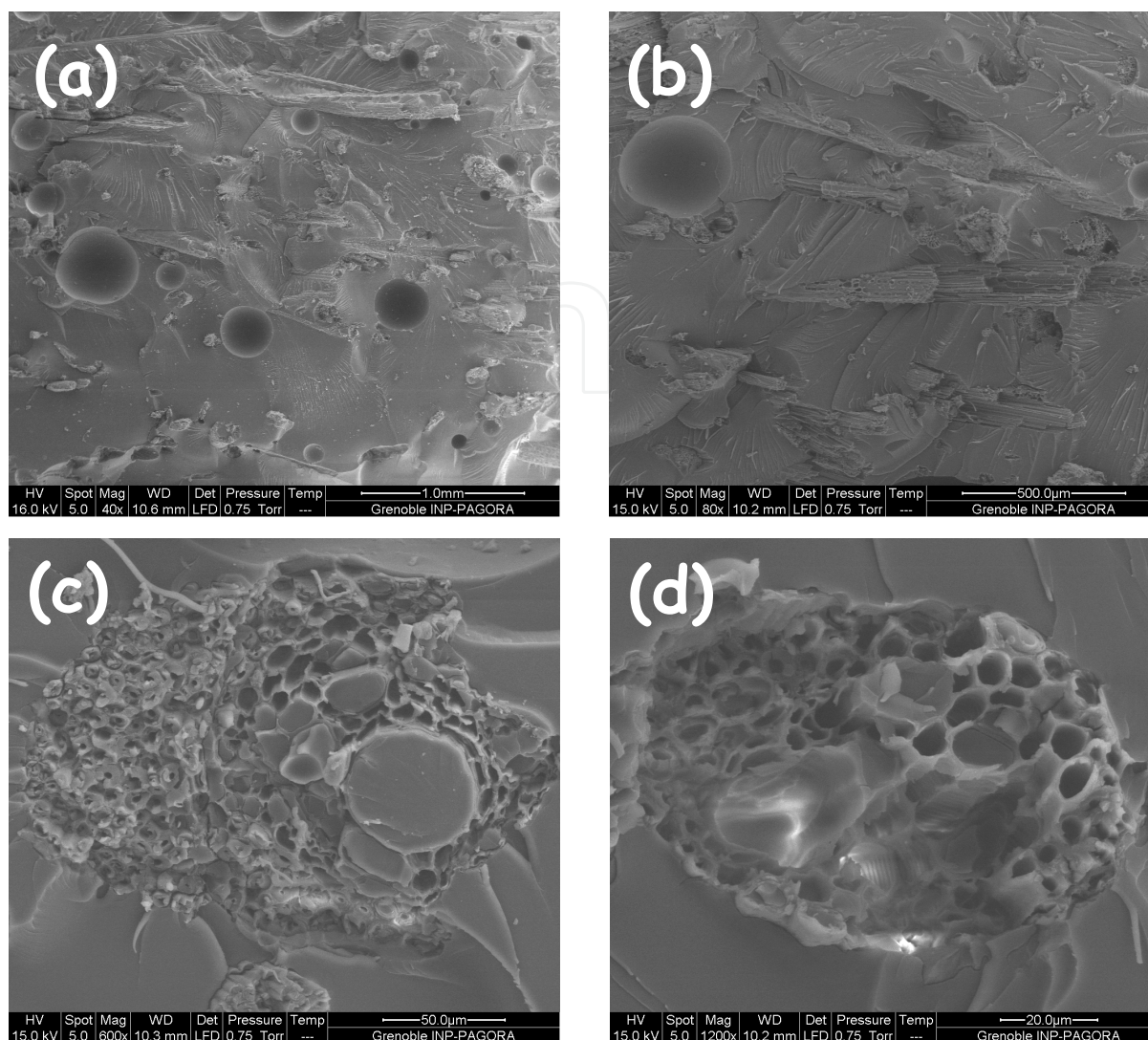
**Figure 10.** Scanning electron micrographs of freshly fractured surfaces of polyepoxy /modified fiber composites with 10 wt % of modified date palm tree fibers at various magnifications.

| Sample | | $T_g$ | $T\alpha$ | $G'_c$ | $G'_c/G'_m$ |
|---|---|---|---|---|---|
| | | °C | °C | Mpa | |
| Neat epoxy | | 155 | 150 | 9.69 (G'e) | 1 |
| Composites based on unmodified fibers | 5 wt% | 147 | 148 | 14.4 | 1.49 |
| | 10 wt% | 148 | 148 | 22.2 | 2.29 |
| | 15 wt% | 145 | 149 | 25.9 | 2.67 |
| Composites based on oxidized fibers | 5 wt% | 147 | 146 | 11.5 | 1.19 |
| | 10 wt% | 137 | 145 | 17.8 | 1.84 |
| | 15 wt% | 137 | 148 | 16.4 | 1.69 |

**Table 4.** The Glass Transition Temperature, Tg, Determined from DSC Measurements, the Main Relaxation Temperature, Tα, the Rubbery Storage Shear Modulus at Tg + 50 °C, the $G'_c$, of the Composite Materials and the Relative Shear Modulus, $G'_c/G'_m$ (where $G'_m$ refers to the rubbery shear storage modulus of the neat epoxy) Determined from DMA Experiments

### 3.2.5. Mechanical behavior

The mechanical behavior of all specimens was investigated under both linear (DMA measurements), non-linear conditions (three-point bending experiments), and Charpy impact tests.

### 3.2.5.1. Dynamical mechanical analysis

The dependence of log G′, i.e. the logarithm of the shear storage modulus, and the loss factor tanδ, vs. the temperature at 1Hz are displayed in Figs. 11 and 12, for composite materials based on unmodified and modified fibers, respectively.

All materials exhibited a relaxation process that was associated with the glass-rubber transition of the matrix, displayed as a sharp decrease in modulus and a concomitant maximum of the loss factor. This relaxation process, denoted α, involved the release of cooperative motions of the chains between crosslinks. The relaxation temperature, Tα, corresponding to the maximum of the loss factor is listed in Table 3, and was found to be approximately 150°C for all materials. A slight decrease in Tα was observed for the composites based on modified fibers; however it was less significant than the one observed for theTg, as obtained by DSC.

From the dependence of log G′ vs. temperature, it was clear, for both kinds of fibers (oxidized and not oxidized), that the modulus at the rubbery state increased with the fibers content. However, it was difficult to observe any significant effect of the filler at low temperature, i.e. in the glassy state. A simple mixing rule rendered it possible to account for this fact. As is well known, the exact determination of a sample's glassy modulus depends on the precise knowledge of the sample dimensions. On the other hand, the water absorption could affect the exact determination of the glassy modulus. Therefore, the reinforcing effect of the filler was estimated in the rubbery region of the polymer matrix. The values of the rubbery shear modulus are reported in Table 4, as are the relative rubbery modulus values corresponding to the ratio of the rubbery modulus of the composites, G′c, divided by that of the neat matrix, G′m . Since the modulus was not perfectly constant as a function of the temperature, the G′ values reported in Table 3 correspond to averages.

For all the composites, the reinforcement effect of the lignocellulosic filler (modified or unmodified) was observed in the rubbery sate. It could be quantified through the values of the relative rubbery modulus, which increased up to 1.84 and 2.67, respectively, for the composites based on the modified and unmodified fibers. The increase in modulus upon filler addition was ascribed to the difference between the modulus of the neat matrix (polyepoxy) and that of the lignocellulosic fibers, as well as to the decent interactions at the interfaces of these composites. No significant effect of the fiber modification was observed on the rubbery modulus despite the fact that TEM microscopy demonstrated the presence of better interactions at the interface in the case of the composites based on modified fibers.
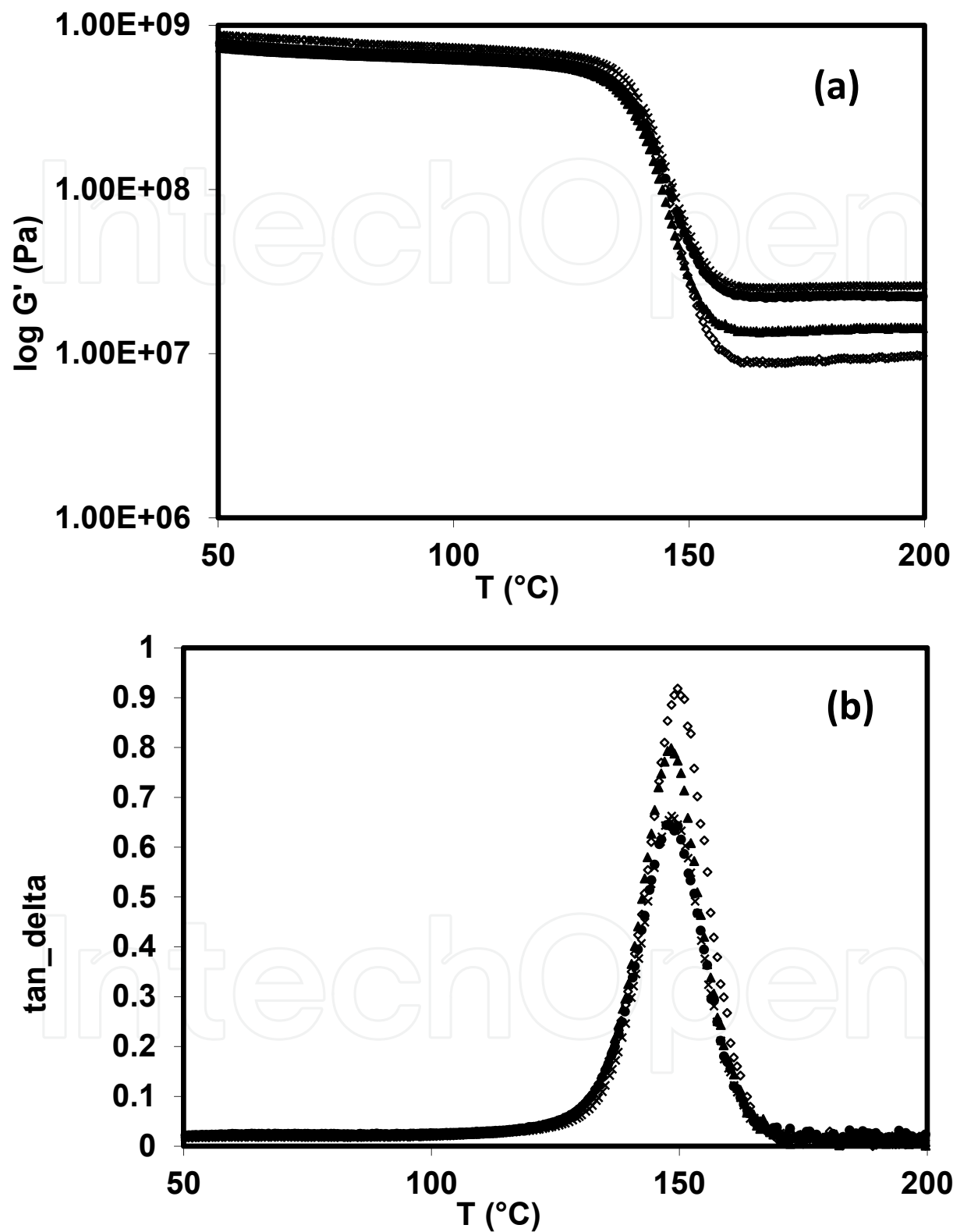
**Figure 11.** (a) The shear storage modulus G₀, and (b) the loss factor tanδ vs. temperature at 1 Hz for composites based on unmodified date palm tree fibers with (◊) 0, (▲) 5, (●)10 and (X) 15 wt.-% of filler
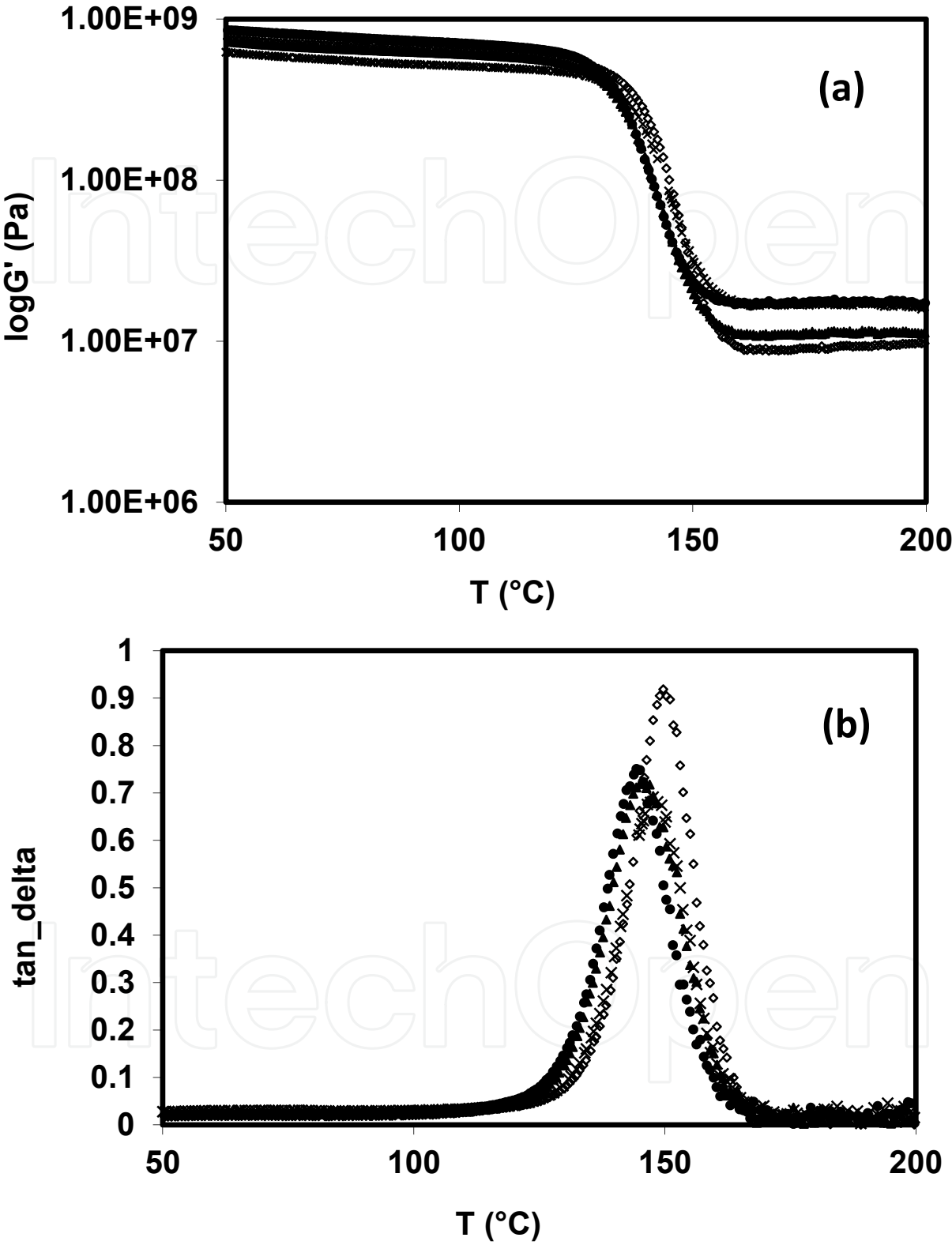
**Figure 12.** (a) The shear storage modulus $G_o$, and (b) the loss factor tan$\delta$ vs. temperature at 1 Hz for composites based on modified date palm tree fibers with ($\Diamond$)0, ($\Delta$) 5 , (O) 10, and (X) 15 wt.-% of filler.

*3.2.5.2. High strain behavior (three-point bending test)*

Storage shear modulus values measured through DMA experiments were determined at room temperature. High strain experiments should provide information on the mechanical properties at the glassy state. Figure 13 gives typical load vs. displacement curves obtained from the three-point bending experiments for the neat polyepoxy matrix and composites filled with 15 wt.-% of modified and unmodified date palm tree fibers. These curves were obtained in the glassy state of the matrix, and the tests were conducted for all materials filled with 5, 10, and 15 wt.-% of modified and unmodified date palm tree fibers. The mechanical properties derived from these experiments are presented in Fig. 14.

Panels a and b of Fig. 14 show the evolution of the shear modulus and the upper yield stress as a function of the filler content. The data were obtained from the three point bending tests. As expected, the composites were more brittle than the neat matrix. The composite material reinforced with the modified filler displayed higher mechanical properties as compared to the composite filled with the unmodified filler. In fact, the composites with modified fibers showed a higher modulus and a higher upper yield stress.
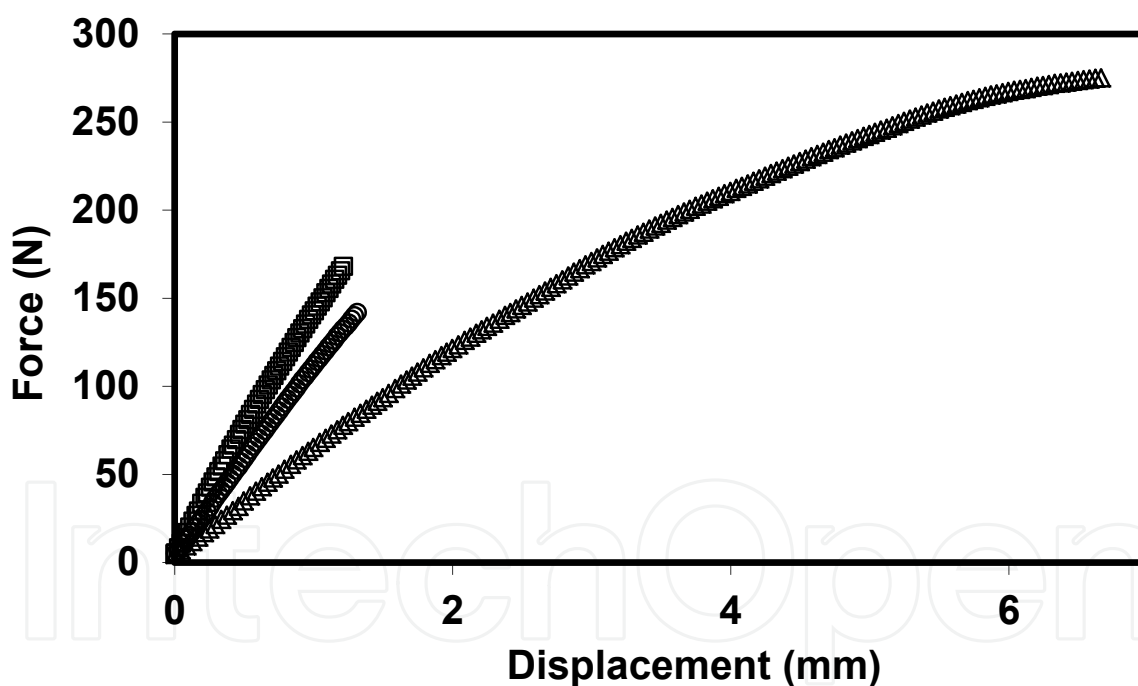


**Figure 13.** Load versus displacement curves obtained from three-point bending tests performed at room temperature (25 °C) for epoxy-based composites filled with : (Δ) 0, (O)15wt% of non-modified fibers and (◊)15 wt % of oxidized palm tree fibers.

*3.2.5.3. Charpy impact tests*

Figure 15 shows the results of Charpy impact tests. The absorbed energy at break is presented as a function of the filler content. These tests confirmed that the composites were brittle. In fact, a lower energy was required for breaking the composite materials as compared to the

neat matrix. On the other hand, and within the error margins, no significant difference was observed between the composites based on modified and unmodified fibers.
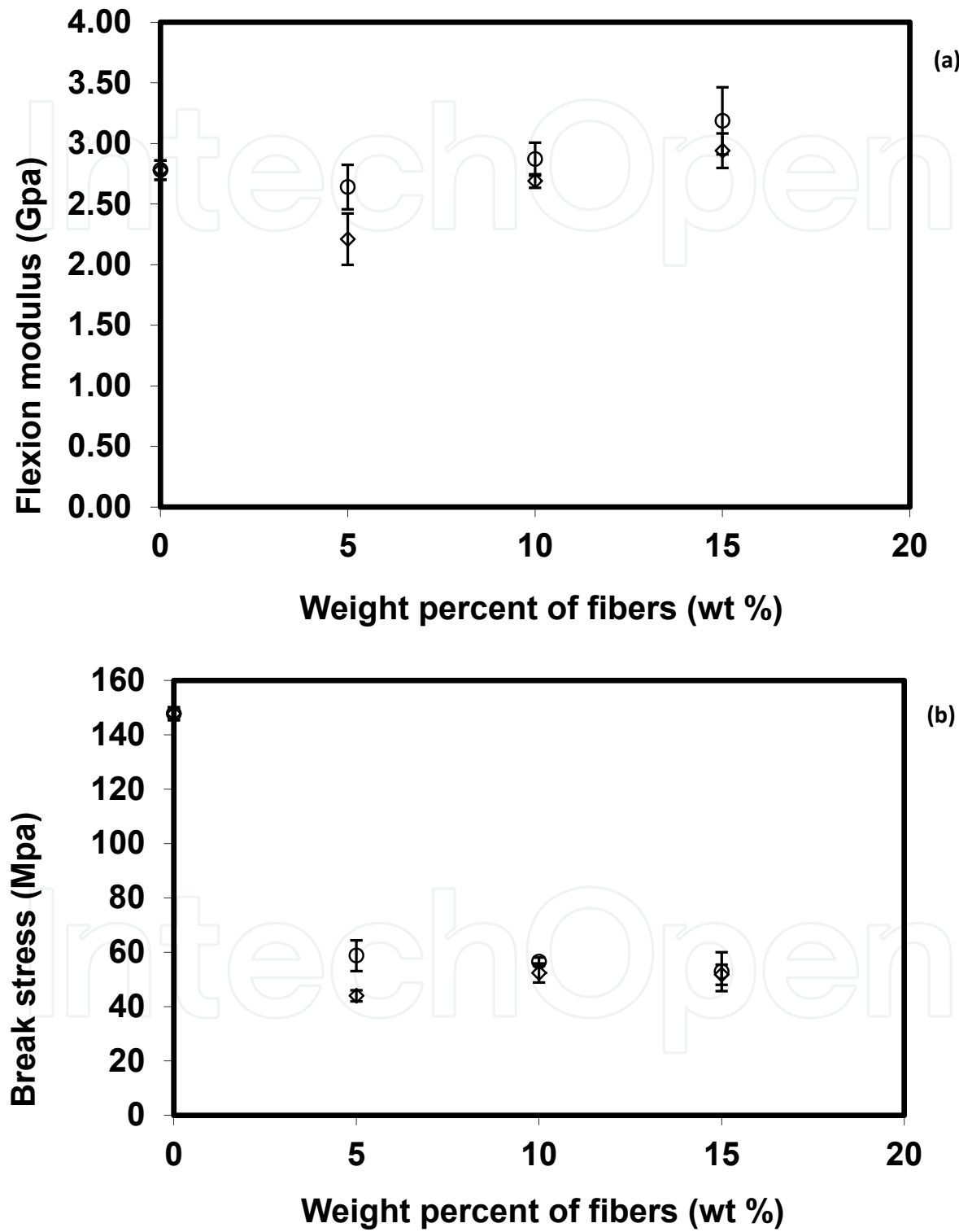


**Figure 14.** Mechanical properties as functions of the filler content, obtained from three-point bending tests of epoxy based composites filled with (O) modified and (◊) unmodified. a) Shear modulus; b) upper yield stress
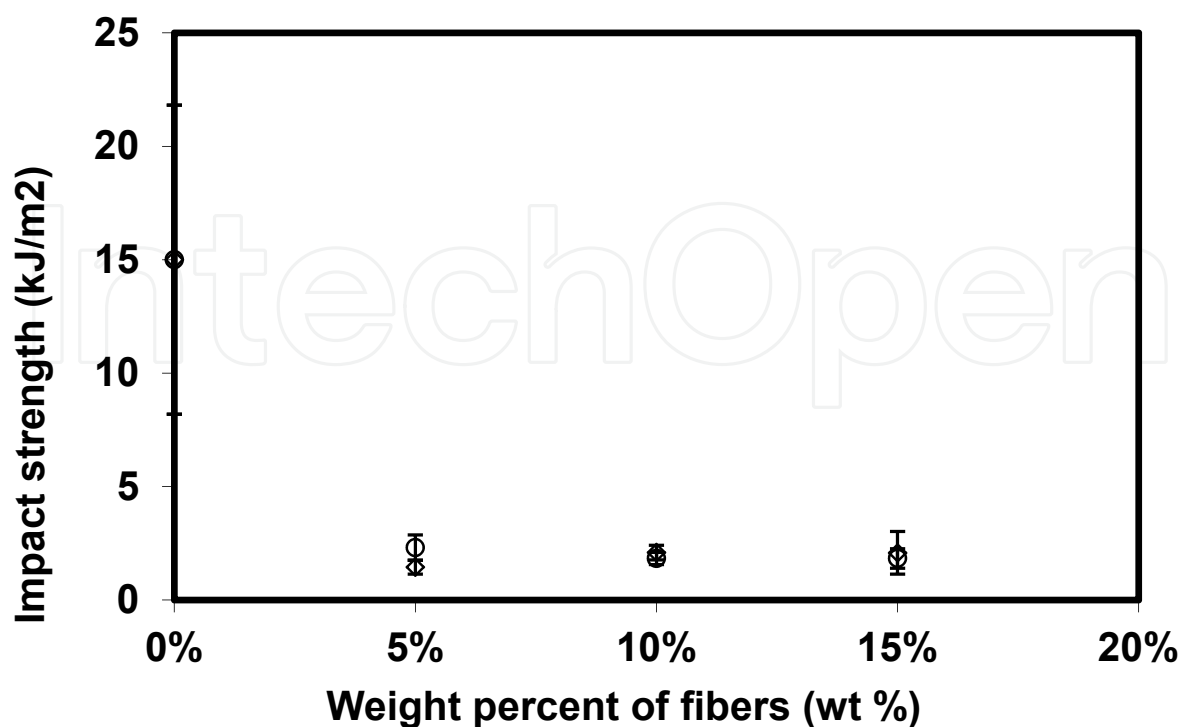
**Figure 15.** The absorbed energy as a function of the filler content, obtained from Charpy impact tests of epoxy based composites filled with (O) modified and (◊) unmodified fibers fibers

## 4. Part 3: Rheokinetic study of the reactive composite materials

### 4.1. Experimental section - Technical Analysis

#### 4.1.1. Differential Scanning Calorimetry (DSC)

A Mettler Thermoanalyser TA3000 operating in the -100°C to 300°C temperature range and equipped with a liquid nitrogen cooling system, was used to determine the enthalpy of reaction, the glass transition temperature $T_g$, which was taken as the onset temperature of the deflection heat capacity change, and variation of the heat capacity $\Delta Cp$ through the $T_g$ of the samples. The heating rate was 10 °C min-1 in a nitrogen atmosphere (flowrate10 mL min-1). The $T_{g0}$ and the heat capacity of the initial unreacted mixture $\Delta Cp_0$ were determined during a first scan, the fully cured material glass transition temperature $T_{g\infty}$ and its corresponding heat capacity change $\Delta Cp_\infty$ were obtained after curing at 160 °C with vaccum.

Isothermal cures were examined at various reaction times. The Conversion, x, can be deduced from DSC Scans and calculated from the following equation:

$$X(t) = 1 - \frac{\Delta H_r(t)}{\Delta H_0}$$

Where $\Delta Hr(t)$ residual heat of reaction and $\Delta H_0$ total enthalpy of the reaction.

### 4.1.2. Rheokinetic study

The gel time was studied by a Couette Rheometer called Rheomat 115 (Cf. Table 5) with a shear rate of 1 s$^{-1}$ and a period of 30 to 60 minutes. The principle of the apparatus is to measure the viscosity of the mixture as a function of time. The sample in liquid form is placed in a cylindrical tube and the bucket used is the one called D.

| Mode | Temperature | Sensors | Frequency | Tools |
|---|---|---|---|---|
| - Viscosity versus shear rate<br>- Time study | T$_{max}$ = 100°C | - Viscosity from 1 mPa.s to 5. 10$^5$ Pa.s<br>- Shear stress from 2 Pa to 35.10$^3$ Pa | - N : from 5 to 780 min$^{-1}$<br>- N/100 : from 0,05 to 780 min$^{-1}$ | 2 bucket used C & D. |

**Table 5.** Rheometer characteristics

## 4.2. Results and discussions

### 4.2.1. Thermal characteristics

#### 4.2.1.1. Epoxy filled by unmodified fibers

To cure thermoset polymers it's important to have information about the thermal properties of the starting monomers but also of the fully cured polymer. On the other hand, in order to understand the final morphology and properties, the study of the evolution of the glass transition during the network formation is of great interest. Thus, the glass transition temperature (Tg) of the epoxy networks based on DPLF fibers (from 5 % wt to 15 % wt) epoxy blends was investigated using DSC analysis. Table 6 lists the experimentally obtained values of Tg$_0$, Tg$_\infty$, $\Delta$Cp$_0$, $\Delta$H$_0$ (relative to the mass of the reactive system), $\Delta$Cp$_\infty$ and $\lambda$ (defined as ratio of $\Delta$Cp$_0$ and $\Delta$Cp$_\infty$) for each DGEBA/IPD /fibers DPLF blend studied. Not that the ratio is still stoichimetric.

| Material | Tg$_0$ (°C) | $\Delta$Cp$_0$ (J.g$^{-1}$.K$^{-1}$) | $\Delta$H$_0$ (J/g) | Tg$_\infty$ (°C) | $\Delta$Cp$_\infty$ (J.g$^{-1}$.K$^{-1}$) | $\lambda = \dfrac{\Delta Cp_\infty}{\Delta Cp_0}$ |
|---|---|---|---|---|---|---|
| **Neat epoxy** | -30 | 0,57 | 463 | 152 | 0,28 | 0,49 |
| **Epoxy with 5 % wt of unmodified fibers** | -29 | 0,47 | 420 | 144 | 0,28 | 0,60 |
| **Epoxy with 10 % wt of unmodified fibers** | -30 | 0,52 | 401 | 135 | 0,32 | 0,62 |
| **Epoxy with 10 % wt of TEMPO oxidized fibers** | -30 | 0,54 | 413 | 119 | 0,29 | 0,54 |

**Table 6.** Influence of fibers on thermal properties (DSC analysis)

The thermal characteristics found for the neat epoxy are the same order of magnitude as reported by literature (Pichaud, 1997, Pichaud et al. 1999, Nguyen-Thuc 2004). The initial Tg (Tg$_0$) and final Tg (Tg$_\infty$) of the neat epoxy/amine system were −30 °C and 152 °C, respectively. The total exothermic energy of the polymerization reaction $\Delta H_0$ was 463 J g−1 K−1.

The enthalpies of reaction $\Delta H_0$ decrease by introducing an increasing amount of fiber. This decrease can be explained by the change in amine/epoxy stochiometry resulting from etherification reactions. Indeed, the fibers are rich in hydroxyl function and furthermore have an amount of trapped water. Thus it is then possible to envisage a competition between the following reactions:

- Reaction between the oxirane of DGEBA and amine functions of the IPD.
- Reaction between the oxirane of DGEBA and water,
- Etherification reaction of DGEBA oxirane and the fibers hydroxyl functions.

It was not possible to highlight the presence of ether bonds, by Infrared, because the absorption bands are overlapped by those of the cellulose. But the significant decrease of glass transition temperature Tg$_\infty$ observed when DPLF fibers are added could be attributed to the the etherification reactions mentioned above and which have caused the change in local stoichiometry (Garcia-Loera 2002, Pascault et al. 2002). The evolution of the glass transition temperature was also observed in the case of epoxy network modified with thermoplastic (Fernandez et al. 2001). On the other hand, the ratio $\lambda$ which characterizes the variation of the chain mobility between the crosslinked polymer and initial monomer, varies from 0.49 to 0.62 when the rate of virgin fiber is from 0 to 10 wt% respectively. This is another indication of the evolution of the polymer network stiffness, caused by the introduction of the fibers and indicates that the fibers induce a variation of the stoichiometric ration (oxirane/amine). These evolutions were not observed when epoxy amine system (DGEBA/IPD) was filled by core-shell (probably little or no functionalized) where no/or few reactions were possible between the cross linking polymer and the core-shell (Nguyen-Thuc et al. 2002, 2003 and 2004).

### 4.2.1.2. Epoxy filled by TEMPO oxidized fibers

In the case of a DGEBA / IPD with modified fibers, we observe similar evolutions of the thermal properties were observed (Tg$_\infty$ decreases and the ratio $\lambda$ increases). The same discussion could be done for these materials, however the decrease of Tg$_\infty$ is much more pronounced when compared to unmodified fibers. In this case, the system is more complex compared to the composites of unmodified fibers because the additional reaction between carboxylic acid and oxirane functions. However it's worthy noticing that the oxidized fibers are more hygroscopic than the unmodified one. Actually, the remaining water fraction after drying (at 105°C overnight) is about 8wt% for the oxidized fibers and 6wt% for the unmodified fibers. This result agrees with this obtained by Trindad et al who compared the moisture in the fibers of sugarcane bagasse before (9.5%) and after modification (11%) by oxidation with sodium periodate (Trindad et al. 2004). This remaining amount of water will induce a variation of the stoichiometry and catalyses the etherification reactions (Sherman et al. 2008). This higher amount of remaining water could explain the more pronounced decrease of Tg$_\infty$ in the case of the composites with oxidized fibers.

### 4.2.2. Kinetic behaviour

The reaction kinetics of the DGEBA / IPD reactive system (r = 1) filled with 0 and 10 wt% unmodified fibers and with oxidized fibers, was studied by DSC. The increase in conversion (the extent of reaction) was monitored as a function of time and curves are plotted in fig. 16.
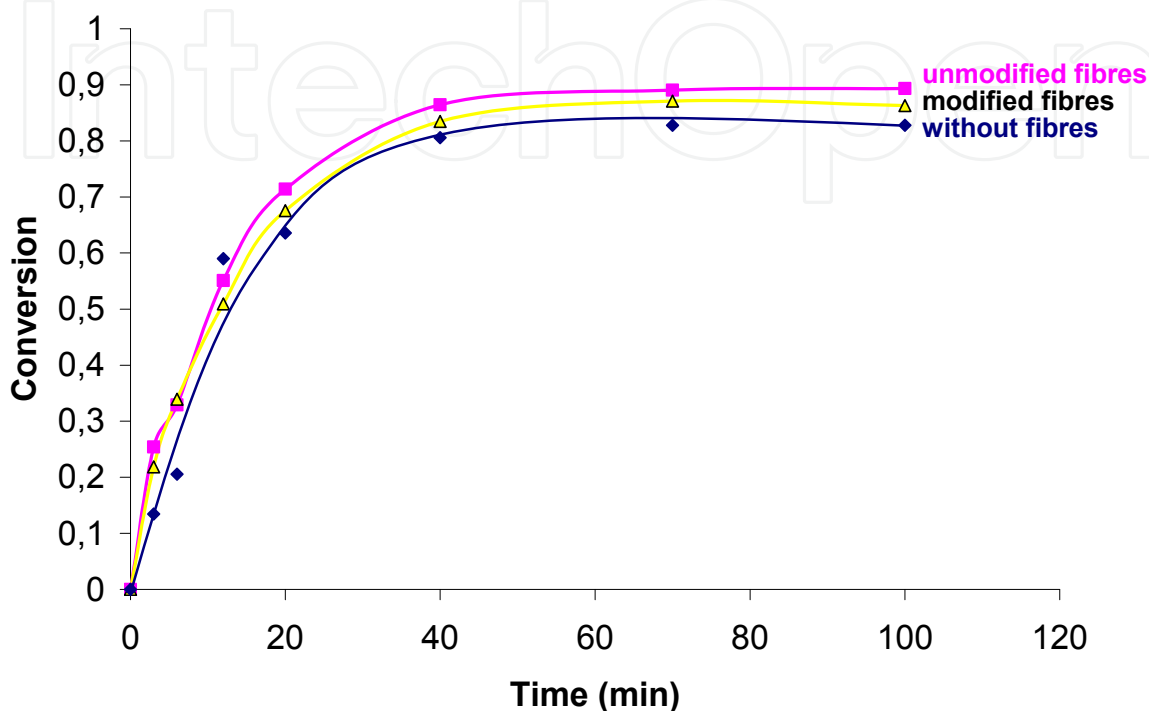


**Figure 16.** Evolution of Conversion x versus time of reaction at 80 °C of system DGEBA / IPD (♦) without fiber (■) with 10% wt of unmodified fibers and (Δ) with 10% wt of TEMPO oxidized fibers

Conversion values are higher for systems with PLD fibers. The polymerization kinetics is enhanced through the presence of these fibers. Indeed the introduction of hydroxyl groups (OH, COOH, H2O ...) in the reaction medium promotes interactions between the epoxy-amine and other nucleophilic molecules leading to the formation of an intermediate complex (Fig 17.) (Rozenberg 1986, Garcia-Lorea 2002).
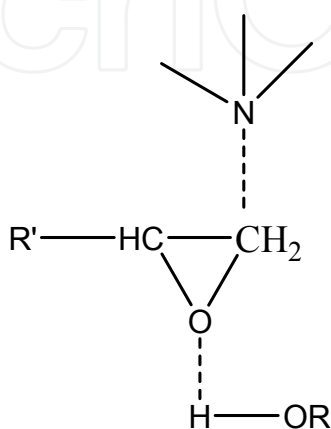


**Figure 17.** Trimolecular complex catalyst formed by hydroxyl functional groups

The formation of this complex makes nucleophilic attack of the primary amine easier and therefore the reaction is accelerated. Indeed, DPLF fibers added to the system contain hydroxyl groups in the case of unmodified fibers, and more acid groups in the case of oxidized fibers. Furthermore a significant amount of water is present (humidity between 6 and 8%wt) which has an additional catalytic effect in the reaction medium. The presence of water seems to be the dominant factor more than acid groups which are presented in small amounts in the oxidized fibers. Garcia-Lorea and al. (Garcia-Lorea 2002) studied the catalytic effect of water on the reaction kinetics of the system DER332 DGEBA / Jeffamine D400. They showed that the kinetics accelerates with the rate of water incorporated into the system epoxy / amine. If we compare the evolution of conversion in our case with the results, we can decide on the strong effect of humidity on the kinetics of fiber. Furthermore the rate of water incorporated studied by Garcia-Lorea (6-10%) is similar to the humidity in DPLF fibers (6-8%) (Garcia-Loera 2002).

The isothermal cure reaction of DGEBA–IPD networks at various cure temperatures was studied. The built-up in Tg and the extent of conversion x, during cure were monitored as the crosslinking reaction progressed under isothermal conditions (Pascault et al. 1990). The Tg –x relationship could be expressed based on Dibenedetto's formula. Fig 18 presents the Tg vs conversion for the different DGEBA/IPD /DPLF fiber systems. This evolution is predicted by the model based on Dibenedetto's approach modified by Pascault and William (Pascault et al. 1990) from an extension of the Couchman equation (Couchman 1987).
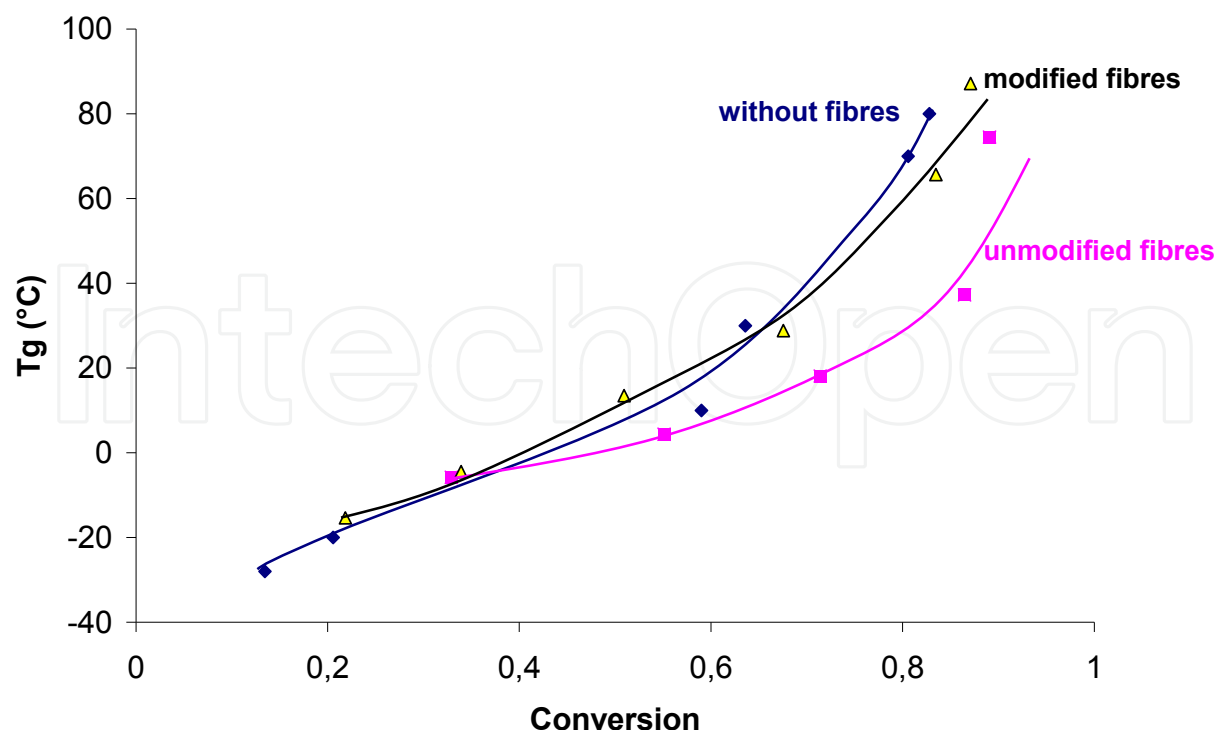


**Figure 18.** Dependence of Tg on conversion x of DGEBA/IPD system at 80 °C of system DGEBA / IPD (♦) without fiber (■) with 10% wt of unmodified fibers and (Δ) with 10% wt of TEMPO oxidized fibers.

$$\frac{Tg - Tg_0}{Tg_\infty - Tg_0} = \frac{\lambda x}{1 - (1 - \lambda)x}$$

They showed that the adjustable parameter $\lambda$ is equal to the ratio $\Delta Cp_\infty / \Delta Cp_0$, where $\Delta Cp_0$ and $\Delta Cp_\infty$ are respectively the heat capacities of the initial mixture and of the fully cured network.

This curve is very important to understand the kinetics of such systems. The correlation between Tg and X characterizes the structure of the reactive system. Three curves are obtained which correspond to the system DGEBA / IPD without fiber, DGEBA / IPD with 10% DPLF fiber and DGEBA / IPD with 10% TEMPO oxidized fiber. At low conversions the Tg values for the system without fiber are lower than those charged by fiber (modified or unmodified). This is due to the nature of chemical reactions that occur. The kinetics are different and the etherification reaction seems to be favoured by the abundance of reactive species (OH fiber, water, and COOH in the case of modified fibers) that catalyzes the crosslinking reaction. From 50% of conversion Tg values of the system without fibers are superior to those systems with fibers (modified or unmodified). In this interval of Conversion, the decrease of Tg was due to the etherification reactions that change the value of stoichiometric ratio (not equal to unity) (Garcia-Loera 2002).

Comparing the two systems, with 10% DPLF fibers and that with 10% TEMPO oxidized fibers, we note that the Tg values are higher for the system based oxidized fibers. This can be explained by the humidity slightly higher in the oxidized fiber and by the existence of carboxylic acid. These conditions make the interpretation of the kinetics very difficult because of competition between many reactive species. It's worthy noticing that in composite materials where the filler doesn't react with the croslinking polymer, Tg-X curves are coincident which indicate that the reaction involved in the croslinking process are the same (Nguyen-Thuc et al. 2003). Thus in our case the fact of the Tg-X curves are not coincident is a proof that the reactions involved in the croslinking process are not the same in the three studied systems and the functional groups of the fibers and water molecules are involved in the croslinking process.

### 4.2.3. Rheokinetic study

We were interested to determine the gelation time of the crosslinking material and to evaluate the effect of fiber on the gel time. The gelation time of the systems DGEBA / IPD with and without DPLF fibers were studied at different temperatures: 60, 70, 80 and 90 °C (Fig.19). These temperatures were chosen above the $Tg_{gel}$ to avoid vitrification (Glass transition) before gelation. According to the work of Pichaud and al (Pichaud et al. 1999) the Tg $_{gel}$ is 32°C for the system DGEBA / IPD.

The gel times determined for the system DGEBA / IPD without fiber are respectively about 30, 14, 9, 5 and 7 minutes at 60, 70, 80 and 90 °C. This result is in parfait agreement with the

results found by Pichaud (Pichaud et al. 1999) with the same system. The fibers induce a reduction of the gelation time and this effect is more exacerbated at mow temperature (60°C). The fibers promote the reaction by the presence of various reactive species, including the catalytic effect which promotes the etherification reactions. This effect is less detectable at high temperatures where the reaction kinetics is much faster.
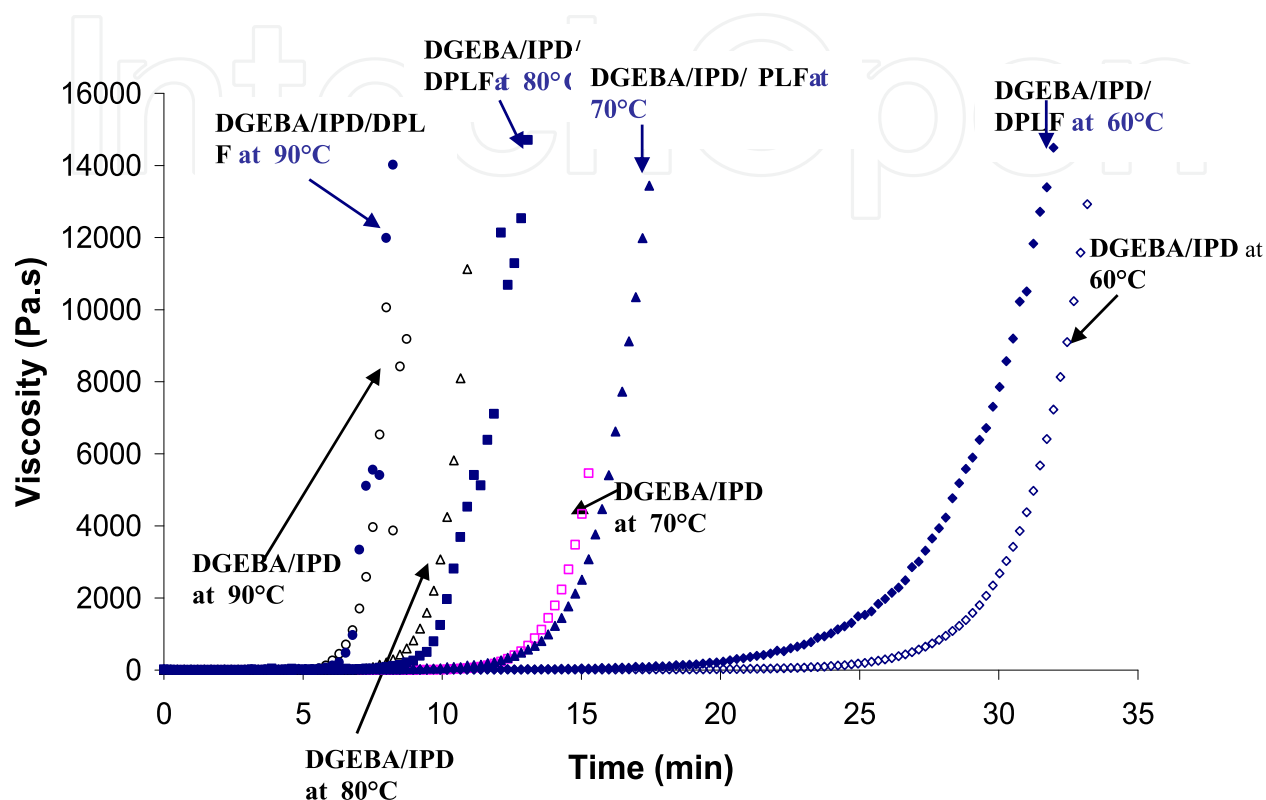


**Figure 19.** Viscosity vs reaction time for the two systems based DGEBA / IPD without fiber and with unmodified fiber to 5% by weight at 60 °, 70 °, 80 ° and 90 °C

The gelation phenomenon was found to obey an Arrhenius law. The value of the activation energy for the system DGEBA / IPD is about 59 kJ / mol. This value is comparable to that obtained in the literature (Ea = 61kJ/mol by Pichaud and al. (Pichaud et al. 1999)). For the system DGEBA / IPD with DPLF fiber, the activation energy is much lower and equal to 47 kJ / mol. This shows that the mechanisms of crosslinking reactions for the system epoxy / amine are not identical because others reactions are induced by the fibers.

*4.2.3.1. Effect of TEMPO oxidized fibers on the gel time*

The fig. 20 below shows the evolution of viscosity versus time for the three systems DGEBA / IPD without fibers (EP), DGEBA / IPD with 5 wt% DPLF fiber and DGEBA / IPD with 5 wt % TEMPO oxidized fibers.

DPLF Fibers into system DGEBA / IPD promotes the reaction kinetics. Nevertheless, viscosity versus time curve of epoxy DGEBA/IPD with oxidized fibers exhibit similar behavior as that with unmodified fibers and the gelation time is the same for both systems (27 min).
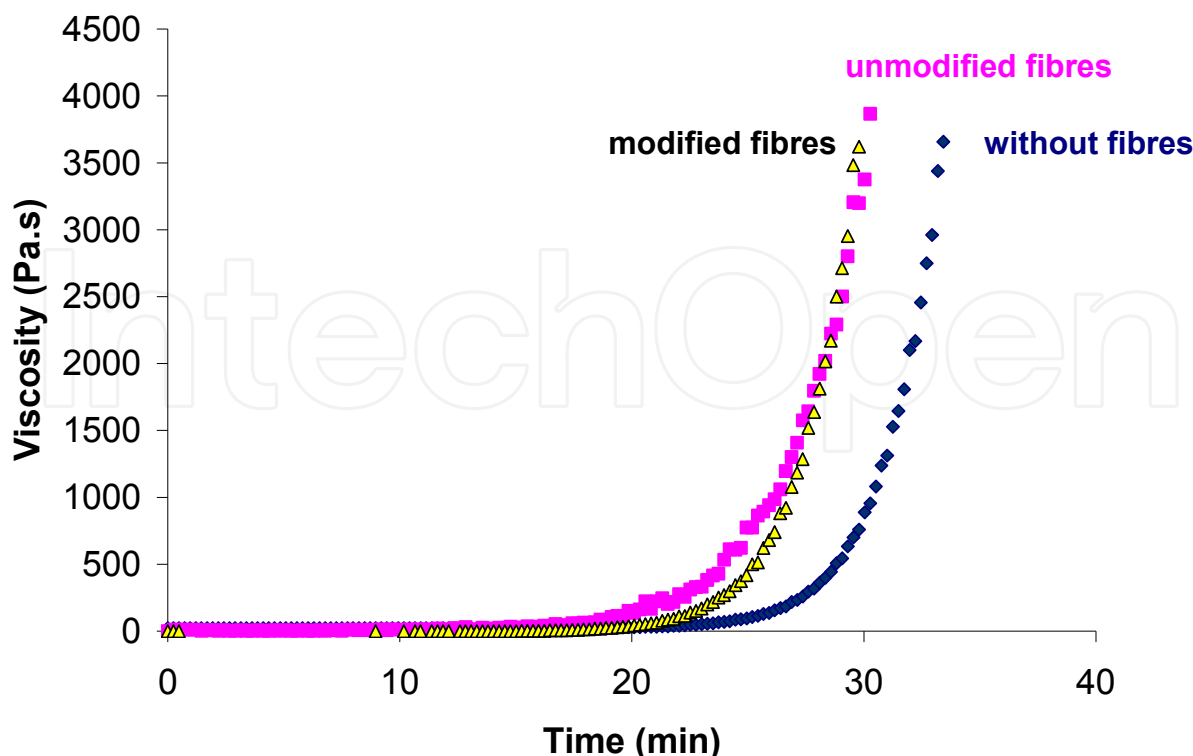
**Figure 20.** Evolution of the viscosity vs reaction time of DGEBA/IPD system at 60 °C (♦) without fiber
(■) with 10% wt of unmodified fibers and (Δ) with 10% wt of TEMPO oxidized fibers.

## 5. Conclusions

The results presented in this study show that date palm lignocellulosic fibers with high lignin and hemicelluloses contents have been successively modified by a classical TEMPO-mediated oxidation process. Despite the composite character of the fibers substrate, kinetic results have proved that oxidation has occurred in a heterogeneous manner. In contrast to previous studies, it was possible to perform this efficient and aqueous chemoselective reaction without destruction of the fibers structure, while keeping a large amount of residual lignin and hemicelluloses. It was further demonstrated that the distribution of the carboxylate group was unconventional, with an inhomogeneity between the core and the surface of the fibers probably due to a migration of the oxidized and partially hydrosoluble product.

The kinetic study by DSC enables to determine the evolution of conversion degree as function of the reaction time. It was also shown that the polymerization kinetics were accelerated in the presence of the fibers. This catalytic effect is more important in the case of the oxidized fibers. This was explained by the presence of water adsorbed by the fibers but also the catalytic effect of the carboxyl groups in the case of the oxidized fibers. However, even the presence of the fibers acceleration the gelation of the system, no effect of the oxidation of the fibers on the gelation time was detected.

When studying the effect of the oxidation on the processing of the composites, it was shown that the preparation of composites using RTM process was facilitated in the case of

composites based on oxidized fibers. During the process, the front displacement of injected resin was regular, homogeneous and faster in the case of oxidized fibers. The morphology, thermal and mechanical properties of polyepoxy reinforced with lignocellulosic fibers extracted from date palm trees were also investigated. Thermal properties from DSC measurements showed that the glass transition temperature of the composites, mainly those based on oxidized fibers, was lower than that of the neat matrix. Dynamic mechanical analysis showed a significant increase of the rubbery modulus when lignocellulosic, unmodified and oxidized fibers were introduced into the polymer. No significant difference of the rubbery modulus between the two families of composites was observed. Analysis of the high strain mechanical proprieties (three-point bending tests) demonstrated some reinforcement of the oxidized fibers as compared to their unmodified counterparts. This confirmed the microscopic analysis which pointed at a better adhesion at the fiber/matrix interface in the case of the composites comprising the oxidized fibers.

## Author details

Adil Sbiai[1,2], Abderrahim Maazouz[2], Etienne Fleury[2], Henry Sautereau[2] and Hamid Kaddami[1]
[1]*Université Cadi Ayyad, Laboratoire de Chimie Organométallique et Macromoléculaire – Matériaux Composites, Faculté des Sciences et Techniques-Guéliz, Morocco*
[2]*INSA, Laboratoire des Matériaux Macromoléculaires / IMP, UMR CNRS n 8 5223, France*

## Acknowledgement

## 6. References

Abdelmouleh M, Boufi S, Salah BA, Belgacem M, Naceur MN, Gandini A (2002) Interaction of silane coupling agents with cellulose. Langmuir 18:3203-3208.

Abu-Sharkh, B. F., and Hamid, H. (2004). "Degradation study of date palm fibre/polypropylene composites in natural and artificial weathering" *Polym Degrad Stab* 85, 967-973.

Bendahou A, Dufresne A, Kaddami H, Habibi Y (2007) Isolation and structural characterization of hemicelluloses from palm of Phoenix dactylifera L. Carbohydr Polym 68: 601–608.

Bendahou A, Kaddami H, Sautereau H, Raihane M, Erchiqui F, Dufresne A (2008) Short palm tree fibers poly olefin composites: Effect of filler content and coupling agent on physical properties. Macromol Mater Eng 293:140-148.

Bendahou A, Habibi Y, Kaddami H, Dufresne A (2009) Physico-chemical characterization of palm from Phoenix Dactylifera-L, preparation of cellulose whiskers and natural rubber-based nanocomposites. J Biobased Mater Bioenergy 3:81-90.

Biagiotti J, Puglia D, Torre L, Kenny JM, Arbelaiz A, Marieta C, Llano-Ponte R, Mondragon I (2004) A systematic investigation on the influence of the chemical treatment of natural fibers on the properties of their polymer matrix composites. Poly Composite 25:470-479.

Bidstrup, S. A., Macosko, C.W. (1986) Structure-Rheology relations for model epoxy networks. 31st International SAMPE Symposium and Exhibition 551-562.

Bin S, Chunju G, Jinhong M, Borun L (2005) Kinetic study on TEMPO-mediated selective oxidation of regenerated cellulose. Cellulose 12: 59-66.

Bledzki AK, Gassan J.(1999)Composites reinforced with cellulose based. Prog Polym Sci 24:221-274.

Chang, P. S., and Robyt, J. F. (1996). "Oxidation of primary alcohol groups of naturally occurring polysaccharides with TEMPO ion," *Carbohydrate Chemistry* 15, 819-830.

Chu, J. (2003) "Development of an intelligent injection system and its application to resin transfer molding," Ph. D. Thesis, McGill University, Montreal, Canada.

Couchman, P. R. (1987) Thermodynamics and the compositional vibration of glass transition temperature, Macromol. 20 : 1712-1717.

Cousin, P., Bataille, P., Schreiber, H. P., and Sapieha, S. (1989). "Cellulose-induced crosslinking of polyethylene," *Journal of Applied Polymer Science* 37(10), 3057-3060.

Coutts, R. S. P., and Campbell, M. D. (1979). "Coupling agents in wood fibre-reinforced cement composites," *Composites* 10(4), 228-232.

Dang Z, Zhang J, Ragauskas AJ (2007) Characterizing TEMPO-mediated oxidation of ECF bleached softwood kraft pulps. Carbohydr Polym 70:310–317.

Da Silva Perez D, Montanari S, Vignon MR (2003) TEMPO-Mediated Oxidation of Cellulose III. Biomacromolecules 4:1417-1425.

Davis, N. J., and Flitsch, S. L. (1993). "Selective oxidation of monosaccharide derivatives to uronic acids," *Tetrahedron Letters* 34, 1181-1184.

De Nooy AEJ, Besemer AC, van Bekkum H (1995) Selective oxidation of primary alcohols mediated by nitroxyl radical in aqueous solution. Kinetics and mechanism. Tetrahedron 51: 8023–8032.

Duanmu J, Gamstedt EK, Rosling A (2007) Hygromechanical properties of composites of crosslinked allylglycidyl-ether modified starch reinforced by wood fibres. Compos Sci Technol 67:3090-3097.

Elazzouzi-Hafraoui S, Nishiyama Y, Putaux JL, Heux L, Dubreuil F, Rochas C (2008) The shape and size distribution of crystalline nanoparticles prepared by acid hydrolysis of native cellulose. Biomacromolecules 9:57-65.

Eloundou, J. P., Feve, M., Gerard, J.F., Harran, D., Pascault, J.P. (1996) Temperature dependence of the behavior of an epoxy-amine system near the gel point through viscoelastic study. 1. Low-Tg epoxy-amine system. Macromol. 29(21) :6907-6917.

Eloundou, J. P., Gerard, J.F., Harran, D., Pascault, J.P. (1996) Temperature dependence of the behavior of a reactive epoxy-amine system by means of rheology. 2. High-Tg epoxy-amine system. Macromol. 29(21): 6917-6927.

Felix, J. M., and Gatenholm, P. (1991). "The nature of adhesion in composites of modified cellulose fibers and polypropylene," *Journal of Applied Polymer Science* 42(3), 609-620.

Felix, F., Gatenholm, P., and Schreiber, H. P. (1994). "Plasma modification of cellulose fibers: Effects on some polymer composite properties," *Journal of Applied Polymer Science* 51(2), 285-295.

Fernandez, B., Corcuera, M.A., Marieta, C., Mondragon, I. (2001) Rheokinetic variations during curing of a tetrafunctional epoxy resin modified with two thermoplastics. Eur.Polym. J. 37:1863-1869.

Flink, P., Westerlind, B., Rigdahl, M., and Stenberg, B. (1988). "Bonding of untreated cellulose fibers to natural rubber," *Journal of Applied Polymer Science* 35(8), 2155-2164.

Fukuzumi, H., Saito, T., Iwata, T., Kumamoto, Y., and Isogai, A. (2009). "Transparent and high gas barrier films of cellulose nanofibers prepared by tempo oxidation," *Biomacromol.* 10, 162-165.

Gandini A (2008) Polymers from renewable resources: A challenge for the future of macromolecular materials. Macromolecules 41:9491-9504.

Garcia-Loera (2002) A. Mélanges réactifs thermodurcissable / Additifs extractibles : Phénomènes de séparation de phase et morphologies. Application aux matériaux poreux, Thèse INSA - Lyon, 161 p.

Gardinera, E. and Cabasso, I. (1987). "On the compatibility and thermally induced blending of poly(styrene phosphonate diethyl ester) with cellulose acetate," *Polymer* 28(12), 2052-357.

Gomez-Bujedo S, Fleury E, Vignon MR (2004) Preparation of cellouronic acids and partially acetylated cellouronic acids by TEMPO/NaClO oxidation of cellulose acetate. Biomacromolecules 5:565-571.

González-Sánchez C, González-Quesada M, De La Orden MU, Urreaga JM (2008) Comparison of the effects of polyethylenimine and maleated polypropylene coupling agents on the properties of cellulose-reinforced polypropylene composites. J Appl Polym Sci 110:2555-2562.

Goussé C, Chanzy H, Cerrada ML, Fleury E (2004) Surface silylation of cellulose microfibrils: Preparation and rheological properties. Polymer 45:1569-1575.

Habibi Y, Chanzy H, Vignon MR (2006) TEMPO-mediated surface oxidation of cellulose whiskers. Cellulose 13:679-687.

Halley, P. J., Mackay, M.E. (1996) Thermorheology of thermosetting-An overview. Polym. Eng. Sci. 36(5) : 593-609.

Han Y, Law K-N, Daneault, C, Lanouette R(2008) Chemical and mechanical techniques for improving the papermaking properties of jack pine TMP fibers. Tappi J 7: 13-18.

Isogai, A., and Kato, Y. (1998). "Preparation of polyuronic acid from cellulose by TEMPO-mediated oxidation," Cellulose 5, 153-164.

Isogai, A., and Saito, T. (2005). "Ion-exchange behavior of carboxylate groups in fibrous cellulose oxidized by the TEMPO-mediated system," Carbohydrate Polymers 61(2), 183-190.

Isogai, T., Yanagisawa, M., and Isogai, A. (2005). "Degrees of polymerization (DP) and DP distribution of cellouronic acids prepared from alkali-treated celluloses and ball-milled native celluloses by TEMPO-mediatedoxidation," Cellulose 16, 117-127.

Iwakura, Y., Kurosaki, T., and Imai, Y. (1965). "Graft copolymerization onto cellulose by the ceric ion method," Journal of Polymer Science Part A: General Papers 3(3), 1185-1193.

Jutier, J.-J., Lemieux, E., and Prud'homme, R. E. (1988). "Miscibility of polyester/ nitrocellulose blends: A DSC and FTIR study," Journal of Polymer Science - Part B: Polym. Phys. 26(6), 1313-1329.

Kaddami H, Dufresne A, Khelifi B, Bendahou A, Taourirte M, Raihane M, Issartel N, Sautereau H, Gérard JF, Sami N (2006) Short palm tree fibers - Thermoset matrices composites. Compos Part A-Appl S 37:1413 – 1422.

Kaliński, R., Galeski, A., and Kryszewski, M. (1981). "Low-density polyethylene filled with chalk and liquid modifier," Journal of Applied Polymer Science 26(12), 4047-3058.

Le Guen MJ, Newman RH (2007) Pulped Phormium tenax leaf fibres as reinforcement for epoxy composites. Compos Part A-Appl S 38:2109-2115.

Levenspiel O (1972) Fluid-particle Reactions in Chemical Reaction Engineering Oregon State University 357-373.

Li Z, Renneckar S, Barone JR (2010) Nanocomposites prepared by in situ enzymatic polymerization of phenol with TEMPO-oxidized nanocellulose. Cellulose 17:57-68.

Manrich, S., and Agnelli, J. A. M. (1989). "The effect of chemical treatment of wood and polymer characteristics on the properties of wood-polymer composites," Journal of Applied Polymer Science 37(7), 1777-1790.

Mao L, Law K-N, Daneault C, Brouillette F (2008) Effects of carboxyl content on the characteristics of TMP fibers. Ind Eng Chem Res 47: 3809-3812.

Mao L, Ma P, Law K, Daneault C, Brouillette F (2010) Studies on kinetics and reuse of spent liquor in the TEMPO-mediated selective oxidation of mechanical pulp. Ind Eng Chem Res 49:113–116.

Martins MA, Forato LA, Mattoso LHC, Colnago LA (2006) A solid state 13C high resolution NMR study of raw and chemically treated sisal fibers. Carbohydr Polym 64:127-133.

Michell, A. J., Vaughan, J. E., and Willis, D. (1978). "Wood fiber-synthetic polymer composites. II. Laminates of treated fibers and polyolefins," Journal of Applied Polymer Science 22(7), 2047-2061.

Mishra S, Mohanty AK, Drzal LT, Misra M, Hinrichsen G (2004) A review on pineapple leaf fibers, sisal fibers and their biocomposites. Macromol Mater Eng 289:955-974.

Moharana, S., Mishra, S. B., and Tripathy, S. S. (1990). "Chemical modification of jute fibers. I. Permanganate-initiated graft copolymerization methyl methacrylate onto jute fibers," Journal of Applied Polymer Science 40(3-4), 345-357.

Montanari S, Roumani M, Heux L, Vignon MR (2005) Topochemistry of carboxylated cellulose nanocrystals resulting from TEMPO-mediated oxidation. Macromolecules 38:1665-1671.

Nguyen-Thuc, B. H., Maazouz, A.,(2002) Morphology and rheology relationships of epoxy/core-shell particles blends. Polym. Eng. Sci. 42:120-133

Nguyen-Thuc, B. H. (2003) Etude rhéocinétique et mécanique des réseaux époxydes modifiés par des élastomères. Mise en forme par le procédé RTM. Thèse INSA-Lyon, 181 p.

Nguyen-Thuc, B. H., and Maazouz, A. (2004). "Elastomer- modified epoxy/amine systems in a resin transfer moulding process," Polymer International 53, 591-602.

Octeau, M.-A. (2001). "Composite bicycle fork design for vacuum assisted resin transfer moulding," Ph. D. Thesis, McGill University, Montreal, Canada.

O'Flynn,J. (2007) "Design for manufacturability of a composite helicopter structure made by resin transfer moulding," Ph. D. Thesis, McGill University, Montreal, Canada.

Okita Y, Saito T, Isogai A (2009) TEMPO-mediated oxidation of softwood thermomechanical pulp. Holzforschung 63: 529-535.

Okita Y, Saito T, Isogai A (2010) Entire surface oxidation of various cellulose microfibrils by TEMPO-mediated oxidation. Biomacromolecules 11:1696-1700.

Pascault, J. P., Williams, R. J. J. (1990) Glass transition temperature versus conversion relashionship for the thermosetting polymers. J. Polym. Sci. Part B : Polymer Physics 28 : 85-95.

Pascault, J. P., Sautereau, H., Verdu, J., Williams, R. J. J. (2002) Thermosetting polymers. New York & Basel, Ed. Marcel DEKKER. 2002.

Paunikallio T, Suvanto M, Pakkanen TT (2006) Viscose fiber/polyamide 12 composites: Novel gas-phase method for the modification of cellulose fibers with an aminosilane coupling agent. J Appl Polym Sci 102:4478-4483.

Philippou, J. L., Johns, W. E., and Tinh, N. (1982). "Bonding wood by graft polymerization. The effect of hydrogen peroxide concentration on the bonding and properties of particleboard," Holzforschung Internat. J. of the Biology, Chemistry, Physics and Technology of Wood 36(1), 37-42.

Pichaud, S. (1997) Etude d'un système réactif époxy-amine en vue du contrôle du procédé d'injection RTM à l'aide de la microdiélectrométrie. Thèse C.N.A.M, 174 p.

Pichaud., S., Duteurtre, X., Fit, A., Stephan, F., Maazouz, A., Pascault, J. P. (1999) Chemorheological and dielectric study of epoxy-amine for processing control. Polym. Inter 48 : 1205-1218.

Raj, R. G., Kokta, B. V., and Daneault, C. (1990). "A comparative study on the effect of aging on mechanical properties of LLDPE-glass fiber, mica, and wood fiber composites," Journal of Applied Polymer Science 40(5), 645-655.

Reich S, El Sabbagh A, Steuernagel L (2008) Improvement of fibre-matrix-adhesion of natural fibres by chemical treatment. Macromol Symp 262:170-181.

Rozenberg, B. A. (1986) Kinetics, thermodynamics and mechanism of reaction of epoxy oligomer with diamines. In: K. Dusek (Ed.). Epoxy resins and composites I. berlin: springer Verlag, Adv. Polym. Sci., Vol. 72, 1986. Kinetics, thermodynamics and mechanism of reaction of epoxy oligomer with diamines 113-165.

Saito T, Isogai A (2004) TEMPO-mediated oxidation of native cellulose. The effect of oxidation conditions on chemical and crystal structures of the water-insoluble fractions. Biomacromolecules 5:1983-1989.

Saito T, Shibata I, Isogai A, Suguri N, Sumikawa N (2005) Distribution of carboxylate groups introduced into cotton linters by the TEMPO-mediated oxidation. Carbohyd Polym 61: 414-419.

Saito T, Hirota M, Tamura N, Kimura S, Fukuzumi H, Heux L, Isogai A (2009) Individualization of nano-sized plant cellulose fibrils by direct surface carboxylation using TEMPO catalyst under neutral conditions. Biomacromolecules 10:1992–1996.

Sakata, I., Morita, M., and Pandey, S. N. (1993a). "Decrystallization of jute by cyanoethylation," *J. Appl. Polym. Sci.* 47(1), 73-83.

Sakata, I., Morita, M., Tsuruta, N., and Morita, K. (1993b). "Activation of wood surface by corona treatment to improve adhesive bonding," *Journal of Applied Polymer Science* 49(7), 1251-1258.

Sapieha, S., Allard, P., and Zang, Y. H. (1991). "Dicumyl peroxide-modified cellulose/LLDPE composites," *Journal of Applied Polymer Science* 41(9-10), 2039-2048.

Sapieha, S., Pupo, J. F., and Schreiber, H. P. (1989). "Thermal degradation of cellulose-containing composites during processing," *Journal of Applied Polymer Science* 37(1), 233-240.

Sbiai, A., Kaddami, H., Fleury, E., Maazouz, A., Erchiqui, F., Koubaa, A., Soucy, J. , and Dufresne, A. (2008). "Effect of the fibers size on the physico-chemical properties of composites based on palm tree fibers and epoxy thermoset polymer," *Macromol. Materials & Engineering* 293(8),684-691.

Sbiai A, Maazouz A, Fleury E, Sautereau H, Kaddami H (2010) Short date palm tree fibers / polyepoxy composites prepared using RTM process: effect of Tempo-mediated oxidation of the fibers. BioResources 5:672-689.

Sbiai, A., Kaddami, H., Sautereau, H., Maazouz, A., and Fleury, E. (2011). "TEMPO mediated oxidation of date palm tree fibers Characterization of modification,".Carbohy. poly.86 (4), 1445-1450.

Segal L, Creely JJ, Martin AE, Conrad CM (1959) An empirical method for estimating the degree of crystallinity of native cellulose using the X-ray diffractometer. Text Res J 29:786-794.

Sherman, C. L., Zeigler, R.C., Verghese, N.E., Marks, M.J. (2008) Structure-property relationships of controlled epoxy networks with quantified levels of excess epoxy etherification. Poly. 49:1164-72.

Shibata I, Isogai A (2003) Depolymerization of cellouronic acid during TEMPO-mediated oxidation. Cellulose 10:151-158.

Sung, N. H., Kaul A., Chin I., and Sung, C. S. P. (1982). "Mechanistic studies of adhesion promotion by γ-aminopropyl triethoxy silane in α-Al$_2$O$_3$/polyethylene joint," *Poly. Eng.and Sci.* 22(10), 637-644.

Tahiri, C., and Vignon, M. R. (2000). "TEMPO-oxidation of cellulose: Synthesis and characterisation of polyglucuronans," *Cellulose* 7, 177-188.

Trindade, W. G., Hoareau, W., Razera, I.A.T., Ruggiero, R., Frollini, E., Castellan, A. (2004 ) Phenolic Thermoset Matrix Reinforced with sugar Cane Bagasse fibers: Attempt to develop a new fiber surface chemical modification involving formation of quinones followed by reaction with furfuryl alcohol. Macromol. Mater. Eng. 289:728-736.

Tzoganakis, C., Vlachopoulos, J., and Hamielec, A. E. (1988). "Production of controlled-rheology polypropylene resins by peroxide promoted degradation during extrusion," *Polymer Engineering and Science* 28(3), 170-180.

Wan Rosli, W. D., Law, K. N., Zainuddin, Z., and Asro, R. (2004). "Effect of pulping variables on the characteristics of oil-palm frond-fiber," *Biores. Technol.* 93, 233-240.

Wikberg H, Maunu SL (2004) Characterisation of thermally modified hard and softwoods by $^{13}$C CPMAS NMR. Carbohyd Polym 58:461-466.

Young, R. A. (1978). "Bonding of oxidized cellulose fibers and interaction with wet strength agents," *Wood and Fiber Science* 10(2), 123-139 .

Zang, Y. H., and Sapieha, S. (1991). "A differential scanning calorimetric characterization of the sorption and desorption of water in cellulose/linear low-density polyethylene composites," *Polymer* 32(12), 489-492.

Zimmermann T, Pöhler E, Geiger T (2004) Cellulose fibrils for polymer reinforcement. Adv Eng Mat 6:754-761.